

# Journal Pre-proof

Netazepide Inhibits Expression of Pappalysin 2 in Type-1 Gastric Neuroendocrine Tumors

K.A. Lloyd, B.N. Parsons, M.D. Burkitt, A.R. Moore, S. Papoutsopoulou, M. Boyce, C.A. Duckworth, K. Exarchou, N. Howes, L. Rainbow, Y. Fang, C. Oxvig, S. Dodd, A. Varro, N. Hall, D.M. Pritchard



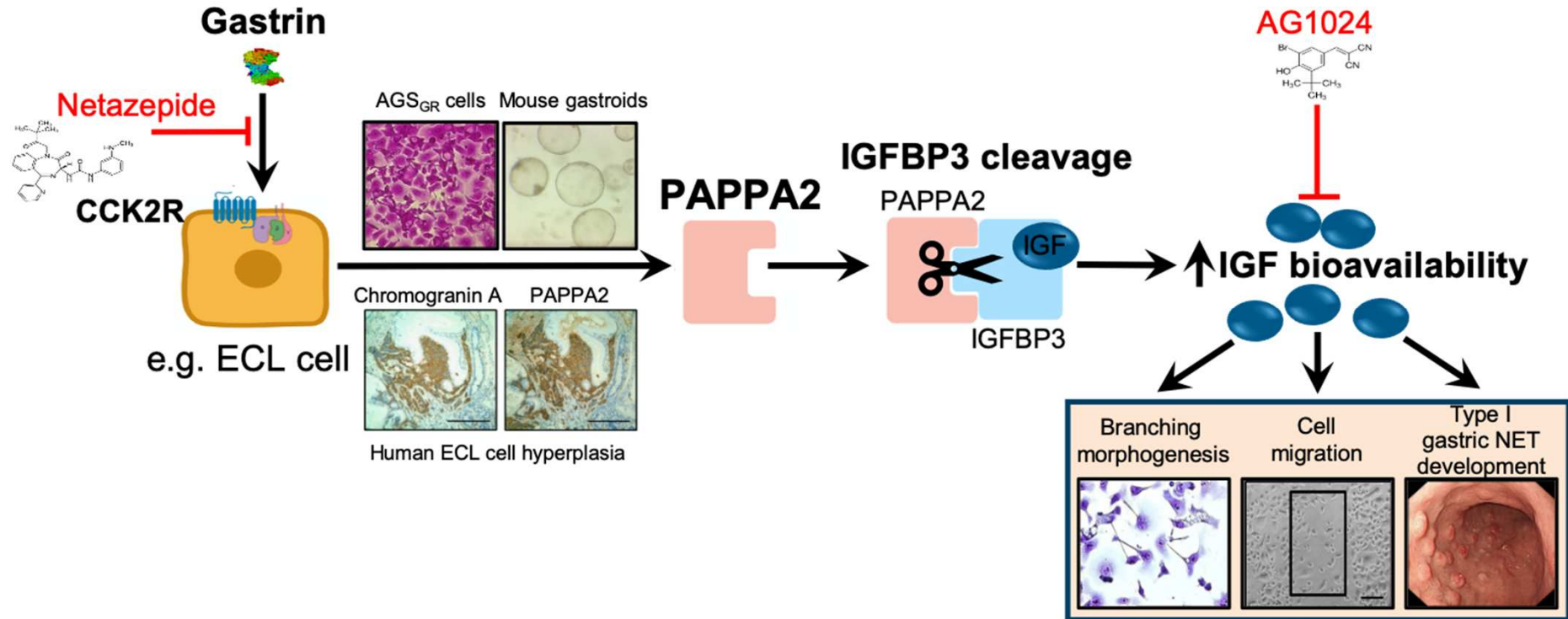
PII: S2352-345X(20)30017-5  
DOI: <https://doi.org/10.1016/j.jcmgh.2020.01.010>  
Reference: JCMGH 576

To appear in: *Cellular and Molecular Gastroenterology and Hepatology*  
Accepted Date: 23 January 2020

Please cite this article as: Lloyd KA, Parsons BN, Burkitt MD, Moore AR, Papoutsopoulou S, Boyce M, Duckworth CA, Exarchou K, Howes N, Rainbow L, Fang Y, Oxvig C, Dodd S, Varro A, Hall N, Pritchard DM, Netazepide Inhibits Expression of Pappalysin 2 in Type-1 Gastric Neuroendocrine Tumors, *Cellular and Molecular Gastroenterology and Hepatology* (2020), doi: <https://doi.org/10.1016/j.jcmgh.2020.01.010>.

This is a PDF file of an article that has undergone enhancements after acceptance, such as the addition of a cover page and metadata, and formatting for readability, but it is not yet the definitive version of record. This version will undergo additional copyediting, typesetting and review before it is published in its final form, but we are providing this version to give early visibility of the article. Please note that, during the production process, errors may be discovered which could affect the content, and all legal disclaimers that apply to the journal pertain.

© 2020 The Authors. Published by Elsevier Inc. on behalf of the AGA Institute.



## **Netazepide Inhibits Expression of Pappalysin 2 in Type-1 Gastric Neuroendocrine Tumors**

**K.A. Lloyd<sup>1\*</sup>, B.N. Parsons<sup>1\*</sup>**, M.D. Burkitt<sup>1</sup>, A.R. Moore<sup>1,2</sup>, S. Papoutsopoulou<sup>1</sup>, M. Boyce<sup>3</sup>, C.A. Duckworth<sup>1</sup>, K. Exarchou<sup>1,2</sup>, N. Howes<sup>2</sup>, L. Rainbow<sup>4</sup>, Y. Fang<sup>4</sup>, C. Oxvig<sup>5</sup>, S. Dodd<sup>1</sup>, A. Varro<sup>1</sup>, N. Hall<sup>4,6,7</sup> and D.M. Pritchard<sup>1,2,8</sup>

<sup>1</sup>*Department of Cellular and Molecular Physiology, Institute of Translational Medicine, University of Liverpool, Crown Street, Liverpool, L69 3GE, UNITED KINGDOM.*

<sup>2</sup>*Liverpool University Hospitals NHS Foundation Trust, Prescot Street, Liverpool, L7 8XP, UNITED KINGDOM.*

<sup>3</sup>*Trio Medicines Ltd, Hammersmith Medicines Research, Cumberland Avenue, London, NW10 7EW, UNITED KINGDOM.*

<sup>4</sup>*Centre for Genomic Research, Institute of Integrative Biology, University of Liverpool, Crown Street, Liverpool, L69 7ZB, UNITED KINGDOM.*

<sup>5</sup>*Department of Molecular Biology and Genetics, Aarhus University, 8000 Aarhus C, DENMARK.*

<sup>6</sup>*The Earlham Institute Norwich Research Park Norwich, Norfolk, NR4 7UH, UNITED KINGDOM.*

<sup>7</sup>*School of Biological Sciences, University of East Anglia, Norwich Research Park, Norwich, Norfolk, NR4 7TJ, UNITED KINGDOM.*

\*Author names in bold designate shared co-first authorship

<sup>8</sup>To whom correspondence should be addressed:

Department of Cellular and Molecular Physiology,  
Institute of Translational Medicine,  
University of Liverpool,  
The Henry Wellcome Laboratory,  
Nuffield Building,  
Crown Street,  
Liverpool  
L69 3GE

Telephone: 0044 151 794 5772

mark.pritchard@liv.ac.uk

**Author contributions**

KAL acquisition of data; analysis and interpretation of data; drafting of the manuscript; statistical analysis

BNP acquisition of data; analysis and interpretation of data; drafting of the manuscript

SP acquisition of data; analysis and interpretation of data; drafting of the manuscript

MDB study concept and design; analysis and interpretation of data; critical revision of the manuscript for important intellectual content; statistical analysis

ARM acquisition of data; critical revision of the manuscript for important intellectual content

MB analysis and interpretation of data; critical revision of the manuscript for important intellectual content

CAD analysis and interpretation of data; critical revision of the manuscript for important intellectual content

KE acquisition of data; critical revision of the manuscript for important intellectual content

NH analysis and interpretation of data; critical revision of the manuscript for important intellectual content

LR acquisition of data; analysis and interpretation of data; critical revision of the manuscript for important intellectual content

YF analysis and interpretation of data; critical revision of the manuscript for important intellectual content; statistical analysis

CO acquisition of data; analysis and interpretation of data; critical revision of the manuscript for important intellectual content

SD acquisition of data; analysis and interpretation of data; critical revision of the manuscript for important intellectual content

AV study concept and design; analysis and interpretation of data; critical revision of the manuscript for important intellectual content; obtained funding; study supervision

NH study concept and design; analysis and interpretation of data; critical revision of the manuscript for important intellectual content; obtained funding; study supervision

DMP study concept and design; analysis and interpretation of data; drafting of the manuscript; critical revision of the manuscript for important intellectual content; obtained funding; study supervision

**Acknowledgements**

This study was funded via a University of Liverpool PhD studentship to KAL, by Trio Medicines Ltd and by the NET Patient Foundation via a TRANSNETS grant. BNP was funded by Worldwide Cancer Research. MDB received financial support from the University of Liverpool and Wellcome Trust Institutional Strategic Support Fund through grant agreement number 097826/Z/11/Z. We thank Dr T.C. Wang (Columbia University, New York) for providing the original colony of INS-GAS mice. Dr M Boyce owns Trio Medicines Ltd, the company developing netazepide as an orphan drug for treatment of gNETs. None of the other authors has any conflicts of interest to declare.

**Article synopsis**

Expression of the metalloproteinase pappalysin 2 (PAPPA2) was inhibited in the stomach of patients with type-I gastric neuroendocrine tumors following treatment with the gastrin/CCK2 receptor antagonist, netazepide. Gastrin-induced PAPPA2 expression in CCK2R expressing gastric epithelial cells resulted in increased insulin-like growth factor (IGF) bioavailability, promotion of cell migration and tissue remodeling.

Journal Pre-proof

## Abstract

**Background & Aims:** In patients with autoimmune atrophic gastritis and achlorhydria, hypergastrinemia is associated with development of type-1 gastric neuroendocrine tumors (gNETs). Twelve months' treatment with netazepide (YF476), an antagonist of the cholecystokinin B receptor (CCKBR or CCK2R), eradicated some type-1 gNETs in patients. We investigated the mechanisms by which netazepide induces gNET regression using gene expression profiling.

**Methods:** We obtained serum samples and gastric corpus biopsies from 8 patients with hypergastrinemia and type-1 gNETs enrolled in a phase 2 trial of netazepide. Control samples were obtained from 10 patients without gastric cancer. We used amplified and biotinylated sense-strand DNA targets from total RNA and Affymetrix Human Gene 2.0 ST microarrays to identify differentially expressed genes in stomach tissues from patients with type-1 gNETs before, during, and after netazepide treatment. Findings were validated in a human AGS<sub>GR</sub> gastric adenocarcinoma cell line that stably expresses human CCK2R, primary mouse gastroids, transgenic hypergastrinemic INS-GAS mice, and patient samples.

**Results:** Levels of papalysin 2 (*PAPPA2*) mRNA were significantly reduced in gNET tissues from patients receiving netazepide therapy compared to tissues collected before therapy. *PAPPA2* is a metalloproteinase that increases bioavailability of insulin-like growth factor (IGF) by cleaving IGF binding proteins (IGFBPs). *PAPPA2* expression was increased in the gastric corpus of patients with type-1 gNETs and immunohistochemistry showed localization in the same vicinity as CCK2R-expressing enterochromaffin-like cells. Upregulation of *PAPPA2* was also found in stomachs of INS-GAS mice. Gastrin increased *PAPPA2* expression with time and in a dose-dependent manner, in gastric AGS<sub>GR</sub> cells and mouse gastroids by activating CCK2R. Knockdown of *PAPPA2* in AGS<sub>GR</sub> cells with small interfering RNAs significantly decreased their migratory response and tissue remodeling in response to gastrin. Gastrin altered the expression and cleavage of IGFBP3 and IGFBP5.

**Conclusions:** In an analysis of human gNETS and mice, we found that gastrin upregulates expression of gastric PAPP2. Increased PAPP2 alters IGF bioavailability, cell migration, and tissue remodeling, which are involved in type-1 gNET development. These effects are inhibited by netazepide.

**KEY WORDS:** tumorigenesis, carcinogenesis, mouse model, hormone, signal transduction

Journal Pre-proof

## Introduction

Gastric neuroendocrine (carcinoid) tumors (gNETs) are relatively rare and originate from enterochromaffin-like (ECL) cells in the oxyntic mucosa of the stomach. They are classified as three types (with an extremely rare fourth type) on the basis of pathological and morphological characteristics[1, 2]. Type-1 gNETs develop as a consequence of the hypergastrinemia that is associated with autoimmune atrophic gastritis, achlorhydria and frequently pernicious anemia. Although type-1 gNETs are usually grade 1 (Ki67 proliferative index <2%) and frequently have an indolent clinical course, 1-20% of patients develop metastases[3, 4] .

The physiological functions of the hormone gastrin have been largely investigated within the stomach, focussing primarily on acid secretion following cholecystokinin type-2 receptor (CCK2R) activation[5]. However, gastrin also plays a central role in regulating gastric tissue remodelling and cell migration[5-10]. These changes are thought to play a role in type-1 gNET development.

Previous studies have suggested that matrix metalloproteinases (MMPs) and insulin-like growth factors (IGFs) play important roles in regulating cellular pathways and thus tumor development in the stomach. Infection with *Helicobacter pylori* (*H. pylori*) increases the production and secretion of MMP7 from gastric epithelial cells[11-13]. Secreted MMP7 liberates insulin like growth factor (IGF)-II from IGFBP-5 (which is released from sub-epithelial cells) and stimulates the expansion and migration of cells in the surrounding gastric microenvironment[14, 15]. Hypergastrinemia also increases gastric MMP7 expression (as well as that of MMP1[7] and MMP9[9]), and this is thought to promote type-1 gNET development via a similar mechanism[10, 14, 15].

Small localised type-1 gNETs can often be successfully removed endoscopically[2]. However in many cases, complete endoscopic resection is not possible due to polyp multiplicity. Therefore, other methods of treatment sometimes need to be considered. Antrectomy can be effective by removing gastrin-secreting G-cells [16], but this involves invasive surgery. Small case series have also reported

benefits from using long-acting somatostatin analogues[17, 18]. However, most recent attention has been given to the potential role of a gastrin/CCK2R antagonist.

Netazepide (YF476) at a concentration of 500 $\mu$ mol/kg has been shown to inhibit ECL cell hyperproliferation and spontaneous type-1 gNET development in African cotton rats (*Sigmodon hispidus*)[19] and *Mastomys* rodents (*Praomys natalensis*)[20]. Recent clinical trials have also demonstrated that patients with type-1 gNETs who received a single daily dose of netazepide orally showed significant reductions in gNET size and number at both 12 weeks and 12 months[21-23]. Biomarkers of gastric pathology such as chromogranin A (CGA; a biomarker of ECL-cell activity), MMP-7 and histidine decarboxylase (HDC) were also suppressed during therapy, while serum gastrin concentrations remained unaffected.

The mechanisms by which netazepide induces these effects in type-1 gNET patients however are currently unknown. We therefore performed a transcriptomic study using gastric biopsy samples obtained from patients before, during and after netazepide treatment to investigate the molecular pathways that were altered during therapy with this drug. One of the mRNAs that showed significant changes in expression was PAPP2. As this protein is known to promote IGF bioavailability in other tissues[24], and as IGFs have a proven involvement in gastric tumorigenesis[14, 15], we concentrated our subsequent analyses on this protein.

## Results

### **Netazepide alters the expression of several genes in hypergastrinemic patients with type-1 gNETs**

Microarray analysis identified several clusters of genes that were differentially expressed in the gastric corpus of hypergastrinemic patients with type-1 gNETs taken before, during (6 and 12 weeks) and 12 weeks after a 50mg oral daily dose of netazepide (Figures 1A and 1B). Of these, clusters 1 and 7 increased after withdrawal of netazepide (Figure 1C) and clusters 10, 13 and 14 showed a significant decrease in expression whilst patients were taking netazepide (weeks 6 and 12), which returned to pre-treatment levels after treatment withdrawal (Figure 1D). Netazepide-inhibited genes within this group included: glycoprotein hormones alpha polypeptide (GHAP), endoplasmic reticulum protein 27 (ERP27), claudin-10 (CLDN10), miRNA-487b (MIR487B), Charcot-Leyden crystal galectin (CLC), secretogranin II (SCG2), peptidyl-glycine alpha-amidating mono-oxygenase (PAM), monoamine oxidase B (MAOB), pappalysin-2 (PAPPA2), tryptophan hydroxylase 1 (TPH1), chromogranin A (CHGA) and histidine decarboxylase (HDC). A list of the most upregulated and downregulated genes after 12 weeks of netazepide relative to baseline is shown in supplementary table 1. We have previously reported significant decreases in the gastric mRNA expression of CHGA and HDC during netazepide treatment[22]. Of the other genes, the highest fold changes were observed with GHAP and PAPPA2. As PAPPA2 is a metalloproteinase that regulates the IGF pathway[24] which is known to be involved in gNET development, this gene/protein was chosen for further investigation.

### **PAPPA2 expression increases in the stomach but not the serum of hypergastrinemic patients with type-1 gNETs**

In gastric corpus biopsies taken from 8 patients with hypergastrinemia and type-1 gNETs, PAPPA2 mRNA abundance was significantly higher at baseline compared to biopsies from 10 healthy normogastrinemic control subjects. Gastric PAPPA2 mRNA expression decreased whilst patients were taking 50mg oral daily netazepide, both in the short-term 12 week (Figure 2A) and long-term

12 month studies (Figure 2B). These data supported the previous microarray findings and also confirmed sustained inhibition of gastric PAPP2 mRNA expression by netazepide in the longer 12 month trial.

Immunohistochemical analysis of serial sections indicated localization of PAPP2 in areas of the tissue which also expressed chromogranin A thus representing areas of micronodular ECL cell hyperplasia (Figure 2C) and type-1 gNET (Figure 2D) in human gastric biopsies, suggesting that this protein is specifically upregulated in CCK2R expressing gNET cells. However, circulating PAPP2 concentrations showed no significant differences between hypergastrinemic type-1 gNET patients and healthy controls (Figures 2E and 2F). Immunohistochemical PAPP2 expression was not detected in gastric corpus biopsies taken from the same patient while taking netazepide (Figure 3). These data therefore suggest that gastrin increases the expression of PAPP2 locally in the gastric mucosa, but the increased expression appears not to be significantly reflected in the circulation.

### **Gastrin increases PAPP2 mRNA and protein expression in AGS<sub>GR</sub> cells via the CCK<sub>2</sub> receptor**

To investigate whether gastrin directly affects PAPP2 expression in CCK2R expressing gastric epithelial cells, we used human gastric adenocarcinoma cells that have been stably transfected with the human CCK<sub>2</sub> receptor (AGS<sub>GR</sub>).

PAPP2 mRNA abundance dose-dependently (Figure 4A) and time-dependently (Figure 4B) increased with gastrin treatment (N=3, n=4) and was maximal after 10nM gastrin for 24h. Immunocytochemistry (representative images are shown in Figure 4C) also demonstrated that PAPP2 protein expression increased significantly in AGS<sub>GR</sub> cells in a dose and time dependent manner following gastrin treatment (Figure 4D and 4E). Western blotting confirmed this increase (Figure 4F). Pre-treatment with the CCK<sub>2</sub> receptor antagonist YM022 or netazepide (both at 100nM) completely reversed the increased expression of PAPP2 caused by 10nM gastrin for 24h (Figure 4G).

### **Gastrin stimulates cell growth and increases PAPPA2 expression in mouse gastric organoids via the CCK<sub>2</sub> receptor**

In order to investigate the effect of gastrin on PAPPA2 expression in the context of the mixed cell population of the gastric epithelium, primary mouse gastric organoid cultures were used[25]. Gastrin treatment increased average gastric organoid area in a dose and time-dependent manner. This was significant after 1nM gastrin for 24h and maximal after 10nM gastrin for 24h (Figure 5A). Gastrin treatment also dose- and time-dependently increased PAPPA2 mRNA expression and this was significant after 10nM gastrin for 24h (Figure 5B) (N=3, n=4). A similar increase in immunofluorescent PAPPA2 expression was also observed following gastrin treatment (Figure 6).

Both gastrin-stimulated gastric organoid growth and increased PAPPA2 expression were completely reversed by pre-treatment with CCK2R antagonist drugs YM022 or netazepide (both at 100nM) (Figures 5C and 5D) (N=3, n=4). Representative bright-field images are shown of mouse gastric organoids with and without pre-treatment with CCK2R antagonists drugs YM022 or netazepide (both at 100nM) and with and without 10nM gastrin treatment for 24h (Figure 5E). Similar observations in response to gastrin and CCK2R antagonists were also made in gastroids derived from INS-GAS mice (Figure 5F).

### **PAPPA2 gene expression is significantly increased in the stomach of hypergastrinemic INS-GAS mice**

Gastrin radioimmunoassay showed no significant differences in serum gastrin concentrations between 15 week old transgenic INS-GAS mice, and age and sex-matched FVB/N controls (Figure 7A). However, circulating gastrin concentrations increased with age in the INS-GAS mice and were significantly increased compared with age-matched wild type FVB/N mice at 33 weeks of age (Figure 7B).

Histological analysis confirmed minimal hyperplasia, but no other significant structural differences in the corpus of INS-GAS mice compared with age-matched FVB/N controls at 15 weeks of age (Figure

7C). However, as expected and previously described[26], remodelling of the gastric corpus mucosa with hyperplasia, atrophy and loss of parietal cells was observed in 33 week old hypergastrinemic INS-GAS mice compared with normogastrinemic age-matched FVB/N wild type controls (Figure 7D).

Quantitative PCR analysis of gastric mucosal scrapes showed no significant differences in PAPPA2 mRNA between 15 week INS-GAS mice and wild-type FVB/N controls (Figure 7E). However, PAPPA2 mRNA expression was significantly increased in 33 week INS-GAS mice relative to age matched wild-type FVB/N mice, in keeping with the observed hypergastrinemia and altered gastric corpus histology at this age (Figure 7F).

### **Gastrin-stimulated PAPPA2 expression significantly increases cell structural remodelling and migration**

Immunofluorescence and qPCR were initially used to confirm the optimal experimental conditions for the successful knockdown of PAPPA2 mRNA and protein in AGS<sub>GR</sub> cells. Quantification of PAPPA2 expression by immunofluorescence (Figures 8A and 8B) and qPCR (Figure 8C) showed that PAPPA2 siRNA (25nM, 48h) successfully reduced gastrin-induced PAPPA2 mRNA and protein expression in AGS<sub>GR</sub> cells by >80% and >90%, respectively (N=3, n=4). Scrambled siRNAs had no such effect.

We chose not to test the effects of PAPPA2 inhibition on cell proliferation as gastrin is known to directly inhibit rather than promote the proliferation of AGS<sub>GR</sub> cells[27]. Instead we decided to investigate two other gastrin-induced cellular phenomena that are associated with tumor development.

Gastrin has previously been shown to induce the remodelling of the actin cytoskeleton via the extension of long processes in AGS<sub>GR</sub> cells[6]. Gastrin (10nM for 6h) induced the extension of long processes in AGS<sub>GR</sub> cells. AGS<sub>GR</sub> cells transfected with 25nM PAPPA2 siRNA for 48h showed a significant decrease in the proportion of cells demonstrating the extension of long processes following treatment with 10nM gastrin for 6h ( $P < 0.0001$ ). PAPPA2 siRNA (25nM) alone did not have any significant effect on cell morphology (N=3, n=3). Representative images are shown of AGS<sub>GR</sub> cells

transfected with PAPP2 25nM siRNA with and without 10nM gastrin treatment for 6h to allow visual comparisons of cell morphology (Figure 8D).

Gastrin has also previously been shown to promote the migration of AGS<sub>GR</sub> cells[8]. Gastrin alone (10nM) stimulated AGS<sub>GR</sub> cell migration after 8h. Transfection with PAPP2 siRNA 25nM for 48h had no effect on AGS<sub>GR</sub> cell migration. However, PAPP2 siRNA at a concentration of 25nM for 48h significantly reduced the migratory response of AGS<sub>GR</sub> cells following addition of 10nM gastrin treatment for 8h ( $P<0.0001$ ,  $N=3$ ,  $n=3$ ). Representative images are shown of the migration of AGS<sub>GR</sub> cells transfected with PAPP2 25nM siRNA with and without 10nM gastrin treatment for 8h (Figure 8E).

Conditioned media from PAPP2 secreting cells also increased the migration of AGS<sub>GR</sub> cells, but at the concentration tested the response was of a lower magnitude than that induced by gastrin (Figure 8F).

### **Gastrin increases AGS<sub>GR</sub> cell migration and cellular remodelling in an IGF-dependent manner**

As PAPP2 is known to promote the cleavage of IGFbps, thus altering the bioavailability of IGFs, we investigated components of this signalling pathway using Western blotting and the insulin-like growth factor-1 receptor (IGF-1R) inhibitor, AG1024.

10nM gastrin for 24h stimulated increased expression of intact IGFBP-5 ( $P<0.05$ ) and cleaved IGFBP-3 ( $P<0.01$ ) (Figure 9A and B) in the media of AGS<sub>GR</sub> cells ( $n=3$ ). In order to investigate whether the increased cleavage of IGFBP-3 resulted in increased IGF bioavailability and to what extent this influenced gastrin-induced cellular migration and structural remodelling, we employed the IGF-1R inhibitor AG1024. In the presence of scrambled siRNA, pre-treatment with 3-20 $\mu$ M AG1024 for 20min followed by 10nM gastrin treatment for 6h resulted in significant decreases in the percentage of cells expressing long processes ( $P<0.0001$ ) (Figure 9C, D). Similarly the cellular migration induced by 10nM gastrin for 8h was significantly inhibited by 1-20 $\mu$ M AG1024 ( $P<0.0001$ ) (Figure 9E, F).

Transfection with PAPP2 siRNA (25nM) for 48h resulted in significant partial (approximately 50%) decreases in gastrin-induced AGS<sub>GR</sub> cell remodelling and migration and both these parameters were further and completely decreased by 10-20 $\mu$ M AG1024 pre-treatment ( $P < 0.001$  and  $P < 0.0001$  respectively) (Figure 9C-F). These findings suggest that the actions of gastrin are wholly dependent on IGF-R but that PAPP2 mediated IGFBP cleavage may be partially responsible for this. For an unknown reason AG1024 appeared to result in a small increase in the percentage of cells expressing long processes following transfection with PAPP-As siRNA, but in the absence of gastrin (Figure 9C).

Journal Pre-proof

## Discussion

We have demonstrated that several genes showed reduced abundance in the stomach of hypergastrinemic type-1 gNET patients during treatment with the gastrin/CCK2R antagonist netazepide. Among these were two ECL-cell specific genes, chromogranin A (CHGA) and histidine decarboxylase (HDC), which we had previously demonstrated by qPCR to be reduced in abundance in the gastric corpus during netazepide therapy[22, 23]. Of the other ten genes that also showed significant reductions in abundance during netazepide therapy, several (such as secretogranin II (SCG2) and peptidyl-glycine alpha-amidating mono-oxygenase (PAM)) are already known to be associated with the gastrin signalling pathway. Further investigation all these netazepide regulated genes will eventually be required to investigate the extent to which they individually contribute towards regulating a patient's response to this drug.

We were however intrigued to find that the abundance of the metalloproteinase PAPP2 was significantly reduced in the stomach during netazepide treatment. PAPP2 is known to promote IGF signalling, a critical pathway involved in gastric tumor development. However, PAPP2 has not previously been associated with gastrointestinal disease, gastrin signalling or neuroendocrine tumor development. We therefore focussed the remainder of this current study on this protein.

We showed that PAPP2 expression is increased in the gastric mucosa of hypergastrinemic human subjects (Figure 2) and transgenic mice (Figure 7) and that PAPP2 is expressed in areas which show a high density of CCK2R expressing ECL cells in patients with type-1 gNETs (Figure 2C,D). Gastrin also directly increased PAPP2 expression in a human gastric epithelial cell line (Figure 4) and in primary mouse gastroid cultures (Figure 5,6), again in a CCK2R-dependent manner. One limitation of our experimental approach however is that unlike patients with autoimmune atrophic gastritis, normal mouse gastroids that have been cultured in the absence of immortalized stomach mesenchymal cells are enriched for the stem cell niche and contain very few differentiated cells such as ECL cells[28].

Thus other CCK2R expressing cells may also be involved in regulating PAPP2 expression in this mouse gastroid model system. Moreover, inhibition of PAPP2 expression partly reversed gastrin-induced changes in cell migration and cellular remodelling in AGS<sub>GR</sub> cells (Figure 8). These effects appear to occur due to increased IGF bioavailability and altered IGFBP-3 cleavage appears to contribute (Figure 9). Thus, gastrin directly increases PAPP2 expression in CCK2R-expressing cells in the stomach and this phenomenon appears to be functionally important.

Pappalysin-2 (Pregnancy-associated plasma protein-A2/PAPP2) is an insulin-like growth factor-binding protein (IGFBP) proteinase[24]. It is highly expressed in the placenta and in other tissues such as the gall bladder, kidney and stomach at much lower levels [29]. PAPP2 and its homologue, PAPP1[30] are the only two members of the pappalysin family within the metzincin superfamily of metalloproteinases[31], which also includes the MMPs (matrix metalloproteinases) and ADAMs (a disintegrin and metalloproteinase family of enzymes). All metzincins share the elongated zinc-binding motif (HEXXHXXGXXH), but PAPP1 and PAPP2 are relatively large proteins and contain modules not present in other metzincins, such as the Lin-Notch repeat (LNR) module, which determines PAPP1 substrate specificity[32]. The pappalysins are also distinct from other proteases such as the matrix metalloproteinases in that they do not cleave matrix proteins. The only known substrates of PAPP1 and PAPP2 are subsets of the IGFBPs[30]. Proteolysis of IGFBPs increases the availability of bioactive IGF to activate the IGF-1 receptor. Aberrant IGF signalling has been shown to be associated with cancer development at several sites[33].

*H. pylori* infection and hypergastrinemia have previously been shown to alter gastric IGF signalling and promote gastric tumor development via a related mechanism. Both factors have been shown to stimulate MMP7 secretion by gastric epithelial cells. This MMP7 in turn cleaves IGFBP-5, leading to increased IGF2 bioavailability from subepithelial myofibroblasts. IGF2 acts upon both gastric epithelial and stromal cells to alter the gastric microenvironment and promote tumor development[10-15]. IGFBP-5 upregulation has also been observed in ~50% of gastric cancers[34].

Tissue inhibitors of metalloproteinases (TIMPs) specifically TIMP1, -3 and -4 have been shown to inhibit this process[35]. However, TIMPs do not inhibit the effects of pappalysins.

Our data suggest that in addition to this previously described MMP-7-associated mechanism, hypergastrinemia also stimulates the secretion of PAPPA2 by gastric epithelial cells. The cells involved express CCK2R and in the setting of autoimmune atrophic gastritis these are most likely to be ECL cells. However paracrine signalling mechanisms involving non-CCK2R expressing cells may also be involved. Secreted PAPPA2 selectively cleaves IGFBPs in the stomach, resulting in altered IGF signalling and consequent alterations to important tumor associated parameters such as cell migration. The mechanism is however crucially different to that induced by MMP-7, because the IGFBP family member that is predominantly cleaved by PAPPA2 appears to be IGFBP-3. It is therefore likely that both MMP7 and PAPPA2 lead to contribute to gastrin-induced increased IGF bioavailability in the stomach, particularly as the responses to gastrin shown in Figure 9 were completely inhibited by the IGF-1 antagonist AG1024, but only partially inhibited by PAPPA2 siRNA.

In conclusion our findings suggest the presence of a novel gastrin-regulated signalling pathway that appears to be important during type-I gNET development. Moreover, inhibition of this pathway by netazepide appears to be one mechanism by which this drug results in gNET tumor regression. It will therefore be interesting to investigate whether single nucleotide polymorphisms in the PAPPA2 gene influence gNET pathogenesis or netazepide response. In addition it will also be important to investigate whether this pathway also plays an important role in *H. pylori* associated gastric carcinogenesis, particularly as the premalignant condition of atrophic gastritis is also associated with hypergastrinemia.

## Methods

### Materials

Amidated unsulphated heptadecapeptide gastrin (G17) was from Bachem, YM022 was from Tocris Bioscience and Netazepide was a gift from Trio Medicines Ltd. All other routine supplies were from Sigma unless otherwise stated.

### Human samples

Serum and gastric corpus biopsies were taken with informed consent and ethical approval at several time points from 8 hypergastrinemic patients with type-1 gNETs who were enrolled on studies 1 and 2 of a phase-2 clinical trial involving treatment with netazepide, as previously described[22, 23]. Control samples were obtained with ethical approval from 10 patients who had a normal upper GI endoscopy, normal gastric histology, no histological or serological evidence of *H. pylori* infection, were not taking proton pump inhibitor drugs and who had fasting serum gastrin concentrations <40pM, as previously described[36].

### Mouse samples

All mouse experiments were carried out under UK Home Office project licence approval. Animals were housed in a specific pathogen free facility at the University of Liverpool with access to food and water *ad libitum*. Gastric mucosal scrapes were taken from 15 or 33 week old transgenic hypergastrinemic INS-GAS mice on the FVB/N genetic background[26, 37] and from wild-type FVB/N mice and stored in RNA later<sup>®</sup> solution for gene expression analysis. Additionally, whole stomachs were formalin fixed and paraffin embedded for histology.

### Cell culture

The human AGS<sub>GR</sub> gastric adenocarcinoma cell line that stably expresses human CCK<sub>2</sub>R[27] was cultured in nutrient mixture F-12 Ham's medium supplemented with 10% Fetal Bovine Serum (Gibco), 2mM L-Glutamine and 1% combined antibiotics streptomycin and penicillin. AGS<sub>GR</sub> cells

expressed chromogranin A and VMAT2 proteins and the abundance of both proteins increased following gastrin treatment (Figure 10). The L-WRN cell line that secretes Noggin, R-spondin-3 and Wnt-3a into the medium was purchased from American Type Culture Collection (ATCC® CRL-3276™) and was cultivated in phenol-red free Dulbecco's modified Eagle media (DMEM) supplemented with 10% Fetal Bovine Serum (Gibco), 2mM L-Glutamine, 0.5mg/ml genetecin (Gibco) and 0.5mg/ml hygromycin B (Invitrogen). L-WRN cells were used to generate growth factor containing conditioned media for gastroid culture. All cells were maintained in a humidified atmosphere of 5% CO<sub>2</sub>/95% O<sub>2</sub> in Galaxy R (Wolf Laboratories) incubators at 37°C and AGS<sub>GR</sub> cells underwent antibiotic selection with 2µg/ml puromycin for 7 days before experimentation.

### **Small interfering RNA (siRNA) transfection**

AGS<sub>GR</sub> cells were transfected with SMARTpool ON-TARGET<sub>plus</sub>™ human PAPA2 siRNA or SMARTpool ON-TARGET<sub>plus</sub>™ Non-targeting Pool siRNA (Table 1) for 48h according to the manufacturer's instructions and using DharmaFECT 1 transfection reagent (GE Dharmacon, Lafayette, USA). Cell culture medium was then changed to serum-free medium when 10nM gastrin treatment was applied.

### **Gastric organoid (gastroid) culture**

The stomachs of 12 week old C57BL/6 or INS-GAS mice were removed and washed in ice cold PBS. After removing the forestomach the remaining tissue was cut into 2x1cm sections and placed into ice-cold chelation buffer (5mM EDTA in PBS) for 2h at 4°C with constant agitation. Glands were released in shaking buffer (43.3mM sucrose, 59.4mM sorbitol in PBS) and ~5000 glands were resuspended in 500µl phenol-red free Matrigel (Scientific Laboratory Supplies) containing 50ng/ml epidermal growth factor (EGF), 100ng/ml fibroblast growth factor 10 (FGF10) (from R&D systems) and 10nM G17. Matrigel (50µl) was plated out, using frozen pipette tips, per well of a pre-warmed 24 well plate. Glands were incubated for 20min at 37°C before application of 500µl basal medium containing 50% L-WRN conditioned medium and 50% DMEM/F12 medium containing 2% L-

glutamine, 20mM HEPES, 2% N2 and 4% B27 supplements with 2% primocin and maintained at 5% CO<sub>2</sub>/ 95% O<sub>2</sub> in Galaxy R incubators at 37°C. Medium was replaced every 4 days with fresh growth medium, which is basal medium plus growth factors EGF (50ng/ml), FGF10 (100ng/ml) and G17 (10nM). Gastroids were passaged every 5-7 days. Experiments involving INS-GAS mice utilised gastroids that had previously been cryopreserved.

### **Treatment of gastric organoids**

Organoids were split after 5-7 days' growth in 50µl Matrigel containing growth factors and left to grow in basal media. Gastrin was removed 3 days post-passage for 24h prior to treatment. Gastroids retained viability following withdrawal of gastrin from the culture media for up to 48h (Figure 11). Organoids were initially treated with 0-10nM gastrin for 6-24h to determine a dose response. Then organoids were pre-treated for 20 min with or without YM022 or netazepide (100nM) followed by 10nM G17 for 6-24h. Untreated organoids and treatments of DMSO (1%) or 10nM G17 alone were used as negative, vehicle and positive controls respectively. After treatment, 5 images per well were taken using a Zeiss Axiovert 25 microscope (Carl Zeiss Microscopy) at x10 magnification and organoid area was calculated using ImageJ. Organoids were then washed with ice-cold PBS and harvested using 400µl cell dissociation solution for 1h on ice with constant agitation. Whole organoids were pelleted and stored at -80°C prior to RNA extraction.

### **RNA isolation and reverse transcription**

RNA was extracted from human biopsies using Tri-Reagent as previously described [22]. Total RNA was isolated from cells and mouse tissues using the RNeasy Mini Kit (Qiagen). Eluted RNA was reverse transcribed into cDNA using the miScript RT II Kit (Qiagen) according to the manufacturer's handbook and stored as undiluted cDNA at -20°C prior to real-time PCR.

## Microarray

Samples were hybridised onto the Affymetrix Human Gene 2.0 ST arrays, which provided coverage of >30,000 coding transcripts and >11,000 long intergenic non-coding transcripts according to manufacturer's instructions. Briefly, 200ng RNA was prepared using the Affymetrix GeneChip WT Plus reagent kit and 3.5ug of fragmented and labelled ss-DNA was loaded onto the array. Arrays were hybridised for 16h at 45°C at 60rpm in the Affymetrix hybridization oven 640, then washed and stained on the GeneChip Fluidics station 450 using fluidics script FS450\_0002. Arrays were scanned using the Affymetrix GeneChip scanner 3000 7G and analyses were obtained using the Affymetrix GeneChip Command Control and Expression Console software.

The detection of significant KEGG pathways was conducted using R package 'gage'[38]. The  $\log_2$  FC from W0/W6 (baseline vs week 6) contrast was inputted into gage for significance testing. The default settings were used, except that "same.dir=FALSE" was selected to consider both up and down-regulation together. Significant pathways were detected using the criterion of false discovery rates (FDR) <5%. Data from the microarray analysis can be found at ArrayExpress using accession number E-MTAB-6473.

## Quantitative polymerase chain reaction (qPCR)

Human PAPP2 forward and GAPDH qPCR primer pair sequences were purchased from Eurogentec (Table 1). Gene expression was assessed using Quantitect primer assays with SYBR green. GAPDH was used for normalization, according to the Quantitect Primer Assay Handbook (Qiagen), and samples were run in a real-time LightCycler 480 (Roche). Each sample was run in quadruplicate and analysis used the  $\Delta\Delta C_T$  method for relative quantification.

## Cell migration assays

Transfected or untransfected AGS<sub>GR</sub> cells were grown as confluent monolayers in 24 well plates before a cell-free region was created using a 2 $\mu$ l pipette tip. Cells were washed twice in PBS, then

washed twice in serum-free media before the treatment was applied. Whole cells that had migrated into the denuded region were counted and scratch wound width was measured using a graticule at 0 and 8h post-treatment. Representative images were taken at these times using a Zeiss Axiovert 25 microscope (Carl Zeiss Microscopy).

### **Cell morphology assays**

Transfected or untransfected AGS<sub>GR</sub> cells ( $1 \times 10^4$ /well) were treated with or without 10nM gastrin for 6h. After treatment, cells were fixed using 3:1 methanol: acetic acid and stained with 0.3% crystal violet. The number of cells that presented long processes were counted as a percentage of total cells in 3 reference fields (>100 cells) per treatment and representative images were taken using the Zeiss Axiovert 25 microscope (Carl Zeiss Microscopy).

### **Immunofluorescence**

Transfected or untransfected AGS<sub>GR</sub> cells were seeded onto 13mm diameter coverslips (VWR International Ltd) in 24 well plates and left to adhere for 24h. Mechanically disrupted gastroids were also seeded onto coverslips in 24 well plates and left to adhere for 3 days. Cells and 2D gastroid monolayers were pre-treated with or without CCK2R inhibitors and with or without 10nM gastrin for 24h.

After treatment, samples were washed with PBS, fixed with 4% paraformaldehyde for 30mins and permeabilised with 0.2% PBT (0.03g BSA, 10ml PBS and 20 $\mu$ l Triton-X 100) for 30mins.

For immunofluorescence, samples were blocked in 10% swine serum (Dako) for 45min at room temperature before overnight incubation with rabbit polyclonal anti-Plac3 (PAPPA2) primary antibody (Thermo Fisher Scientific) diluted 1:500 in PBS in a humidified chamber at 4°C. Salt washes were applied before incubation with swine anti-rabbit FITC conjugated secondary antibody (Dako) diluted 1:500 in 1% BSA in PBS for 1h, protected from light. Samples were washed before mounting with Vectashield® mounting media with DAPI (Vectorlabs) onto glass slides for visualization. Images

were captured using the Olympus BX51 fluorescence microscope (Olympus) at 6 reference fields (>100 cells) per treatment, and relative intensities of nuclear and cytoplasmic staining were analysed using AxioVision Rel. 4.8 software. Samples stained with secondary antibody alone were used as non-specific binding controls.

## **Immunohistochemistry**

Immunohistochemistry was performed on 4µm thick formalin-fixed, paraffin-embedded human gastric biopsy sections. Subsequent to deparaffinization, antigen retrieval was performed by microwaving in 10mM citric acid buffer (pH 6) for 20mins for chromogranin A immunohistochemistry only. Endogenous peroxidase activity and nonspecific binding were blocked at 22°C using peroxidase block (Dako) for 5min and protein block (Dako) for 30min, respectively. Tissue sections were incubated with monoclonal mouse primary PAPP A2 antibody (mAb PA257 [39]) or polyclonal rabbit primary CGA antibody (Santa Cruz) diluted in 50mM Tris, 100mM NaCl, 1mM CaCl<sub>2</sub>, 1% BSA, pH 7.4 for 1h at 22°C, followed by horseradish peroxidase (HRP)-conjugated goat anti-mouse or anti-rabbit immunoglobulins (Dako) for 30min at 22°C, and finally developed by incubation with DAB. Immunostained tissues were counterstained with Mayer's hematoxylin (VWR). Separate mouse tissue sections were stained with hematoxylin-eosin (HE) (VWR) and scored for quantitative histological assessment as previously described[40].

## **ELISAs**

PAPP A2 concentrations in serum samples were determined essentially as previously reported using an assay based on two monoclonal antibodies and calibration of the assay with recombinant human PAPP A2[39].

## Gastrin radioimmunoassay (RIA)

Serum gastrin concentration was measured by radioimmunoassay (RIA) using antiserum L2 directed against the C-terminus of all amidated gastrins as previously described [41] [42]. Normal fasting circulating gastrin concentrations are <40pM.

## Western blotting

Media samples from AGS<sub>GR</sub> cells were concentrated using StrataClean resin (Agilent Technologies) and processed as previously described[7]. To assess proteolytic activity, proteins were separated on 15% SDS-polyacrylamide gels and probed using either polyclonal goat IGFBP-3 or IGFBP-5 primary antibodies (R&D systems) at 1:500 followed by rabbit anti-goat horseradish peroxidase (HRP)-conjugated secondary antibody at 1:5000 (R&D systems). Membranes were developed using Supersignal (ThermoFisher) and chemiluminescence was detected using a Bio-Rad ChemiDoc XRS+ (Bio-Rad). Densitometry was performed using ImageLab software (V 3.0).

## Statistics

Data are presented as means or percentage of control  $\pm$ SEM. Either one or two-way ANOVA, as appropriate, with Sidak *post-hoc* test were used to establish statistical significance.  $P < 0.05$  was considered significant. A Mann Whitney-U test was used to assess statistical differences between healthy and gNET patient samples. A Wilcoxon signed ranked test with Bonferroni correction was used to determine significant differences between repeated samples from the same patients and  $P < 0.0125$  was considered significant after correction.

## References

- [1] Burkitt M, Pritchard D. Review article: pathogenesis and management of gastric carcinoid tumours. *Alimentary pharmacology & therapeutics* 2006;24(9):1305-20.
- [2] Delle Fave G, O'Toole D, Sundin A, Taal B, Ferolla P, Ramage JK, Ferone D, Ito T, Weber W, Zheng-Pei Z, De Herder WW, Pascher A, Ruszniewski P, Vienna Consensus Conference p. ENETS Consensus Guidelines Update for Gastroduodenal Neuroendocrine Neoplasms. *Neuroendocrinology* 2016;103(2):119-24.
- [3] Grozinsky-Glasberg S, Thomas D, Strosberg JR, Pape U-F, Felder S, Tsolakis AV, Alexandraki KI, Fraenkel M, Saiegh L, Reissman P, Kaltsas G, Gross DJ. Metastatic type 1 gastric carcinoid: A real threat or just a myth? *World journal of gastroenterology : WJG* 2013;19(46):8687-95.
- [4] Sagatun L, Fossmark R, Jianu CS, Qvigstad G, Nordrum IS, Mjønes P, Waldum HL. Follow-up of patients with ECL cell-derived tumours. *Scandinavian Journal of Gastroenterology* 2016;51(11):1398-405.
- [5] Dockray G, Dimaline R, Varro A. Gastrin: old hormone, new functions. *Pflugers Arch* 2005;449(4):344-55.
- [6] Pagliocca A, Wroblewski LE, Ashcroft F, Noble P, Dockray GJ, Varro A. Stimulation of the gastrin-cholecystokinin receptor promotes branching morphogenesis in gastric AGS cells. *American Journal of Physiology-Gastrointestinal and Liver Physiology* 2002;283(2):G292-G9.
- [7] Kumar JD, Steele I, Moore AR, Murugesan SV, Rakonczay Z, Venglovecz V, Pritchard DM, Dimaline R, Tizslavicz L, Varro A, Dockray GJ. Gastrin stimulates MMP-1 expression in gastric epithelial cells: putative role in gastric epithelial cell migration. *Am J Physiol Gastrointest Liver Physiol* 2015;309(2):G78-86.
- [8] Noble PJ, Wilde G, White MR, Pennington SR, Dockray GJ, Varro A. Stimulation of gastrin-CCKB receptor promotes migration of gastric AGS cells via multiple paracrine pathways. *American Journal of Physiology-Gastrointestinal and Liver Physiology* 2003;284(1):G75-G84.
- [9] Wroblewski LE, Pritchard DM, Carter S, Varro A. Gastrin-stimulated gastric epithelial cell invasion: the role and mechanism of increased matrix metalloproteinase 9 expression. *Biochem J* 2002;365(Pt 3):873-9.
- [10] Varro A, Kenny S, Hemers E, McCaig C, Przemeck S, Wang TC, Bodger K, Pritchard DM. Increased gastric expression of MMP-7 in hypergastrinemia and significance for epithelial-mesenchymal signaling. *Am J Physiol Gastrointest Liver Physiol* 2007;292(4):G1133-40.
- [11] Bebb JR, Letley DP, Thomas RJ, Aviles F, Collins HM, Watson SA, Hand NM, Zaitoun A, Atherton JC. *Helicobacter pylori* upregulates matrilysin (MMP-7) in epithelial cells in vivo and in vitro in a Cag dependent manner. *Gut* 2003;52(10):1408-13.
- [12] Crawford HC, Krishna US, Israel DA, Matrisian LM, Washington MK, Peek RM. *Helicobacter pylori* strain-selective induction of matrix metalloproteinase-7 in vitro and within gastric mucosa. *Gastroenterology* 2003;125(4):1125-36.
- [13] Wroblewski LE, Noble PJ, Pagliocca A, Pritchard DM, Hart CA, Campbell F, Dodson AR, Dockray GJ, Varro A. Stimulation of MMP-7 (matrilysin) by *Helicobacter pylori* in human gastric epithelial cells: role in epithelial cell migration. *J Cell Sci* 2003;116(Pt 14):3017-26.
- [14] McCaig C, Duval C, Hemers E, Steele I, Pritchard DM, Przemeck S, Dimaline R, Ahmed S, Bodger K, Kerrigan DD, Wang TC, Dockray GJ, Varro A. The role of matrix metalloproteinase-7 in redefining the gastric microenvironment in response to *Helicobacter pylori*. *Gastroenterology* 2006;130(6):1754-63.
- [15] Hemers E, Duval C, McCaig C, Handley M, Dockray GJ, Varro A. Insulin-like growth factor binding protein-5 is a target of matrix metalloproteinase-7: implications for epithelial-mesenchymal signaling. *Cancer Res* 2005;65(16):7363-9.
- [16] Gilligan C, Lawton G, Tang L, West A, Modlin I. Gastric carcinoid tumors: the biology and therapy of an enigmatic and controversial lesion. *The American journal of gastroenterology* 1995;90(3):338-52.

- [17] Jianu CS, Fossmark R, Syversen U, Hauso O, Fykse V, Waldum HL. Five-year follow-up of patients treated for 1 year with octreotide long-acting release for enterochromaffin-like cell carcinoids. *Scand J Gastroenterol* 2011;46(4):456-63.
- [18] Fykse V, Sandvik AK, Qvigstad G, Falkmer SE, Syversen U, Waldum HL. Treatment of ECL cell carcinoids with octreotide LAR. *Scand J Gastroenterol* 2004;39(7):621-8.
- [19] Martinsen TC, Kawase S, Håkanson R, Torp SH, Fossmark R, Qvigstad G, Sandvik AK, Waldum HL. Spontaneous ECL cell carcinomas in cotton rats: natural course and prevention by a gastrin receptor antagonist. *Carcinogenesis* 2003;24(12):1887-96.
- [20] Kidd M, Siddique Z, Drozdov I, Gustafsson B, Camp R, Black J, Boyce M, Modlin I. The CCK2 receptor antagonist, YF476, inhibits Mastomys ECL cell hyperplasia and gastric carcinoid tumor development. *Regulatory peptides* 2010;162(1):52-60.
- [21] Fossmark R, Sordal O, Jianu CS, Qvigstad G, Nordrum IS, Boyce M, Waldum HL. Treatment of gastric carcinoids type 1 with the gastrin receptor antagonist netazepide (YF476) results in regression of tumours and normalisation of serum chromogranin A. *Aliment Pharmacol Ther* 2012;36(11-12):1067-75.
- [22] Moore AR, Boyce M, Steele IA, Campbell F, Varro A, Pritchard DM. Netazepide, a Gastrin Receptor Antagonist, Normalises Tumour Biomarkers and Causes Regression of Type 1 Gastric Neuroendocrine Tumours in a Nonrandomised Trial of Patients with Chronic Atrophic Gastritis. *PLoS ONE* 2013;8(10):e76462.
- [23] Boyce M, Moore AR, Sagatun L, Parsons BN, Varro A, Campbell F, Fossmark R, Waldum HL, Pritchard DM. Netazepide, a gastrin/cholecystokinin-2 receptor antagonist, can eradicate gastric neuroendocrine tumours in patients with autoimmune chronic atrophic gastritis. *British Journal of Clinical Pharmacology* 2016:n/a-n/a.
- [24] Overgaard MT, Boldt HB, Laursen LS, Sottrup-Jensen L, Conover CA, Oxvig C. Pregnancy-associated plasma protein-A2 (PAPP-A2), a novel insulin-like growth factor-binding protein-5 proteinase. *Journal of Biological Chemistry* 2001;276(24):21849-53.
- [25] Barker N, Huch M, Kujala P, van de Wetering M, Snippert HJ, van Es JH, Sato T, Stange DE, Begthel H, van den Born M, Danenberg E, van den Brink S, Korving J, Abo A, Peters PJ, Wright N, Poulson R, Clevers H. Lgr5(+ve) stem cells drive self-renewal in the stomach and build long-lived gastric units in vitro. *Cell Stem Cell* 2010;6(1):25-36.
- [26] Wang TC, Dangler CA, Chen D, Goldenring JR, Koh T, Raychowdhury R, Coffey RJ, Ito S, Varro A, Dockray GJ, Fox JG. Synergistic interaction between hypergastrinemia and Helicobacter infection in a mouse model of gastric cancer. *Gastroenterology* 2000;118(1):36-47.
- [27] Varro A, Noble PJ, Wroblewski LE, Bishop L, Dockray GJ. Gastrin-cholecystokinin(B) receptor expression in AGS cells is associated with direct inhibition and indirect stimulation of cell proliferation via paracrine activation of the epidermal growth factor receptor. *Gut* 2002;50(6):827-33.
- [28] Schumacher MA, Aihara E, Feng R, Engevik A, Shroyer NF, Ottemann KM, Worrell RT, Montrose MH, Shivdasani RA, Zavros Y. The use of murine-derived fundic organoids in studies of gastric physiology. *J Physiol* 2015;593(8):1809-27.
- [29] Fagerberg L, Hallstrom BM, Oksvold P, Kampf C, Djureinovic D, Odeberg J, Habuka M, Tahmasebpoor S, Danielsson A, Edlund K, Asplund A, Sjostedt E, Lundberg E, Szgyarto CA, Skogs M, Takanen JO, Berling H, Tegel H, Mulder J, Nilsson P, Schwenk JM, Lindskog C, Danielsson F, Mardinoglu A, Sivertsson A, von Feilitzen K, Forsberg M, Zwahlen M, Olsson I, Navani S, Huss M, Nielsen J, Ponten F, Uhlen M. Analysis of the human tissue-specific expression by genome-wide integration of transcriptomics and antibody-based proteomics. *Molecular & cellular proteomics : MCP* 2014;13(2):397-406.
- [30] Oxvig C. The role of PAPP-A in the IGF system: location, location, location. *Journal of cell communication and signaling* 2015;9(2):177-87.

- [31] Boldt HB, Overgaard MT, Laursen LS, Weyer K, Sottrup-Jensen L, Oxvig C. Mutational analysis of the proteolytic domain of pregnancy-associated plasma protein-A (PAPP-A): classification as a metzincin. *Biochem J* 2001;358(2):359-67.
- [32] Boldt HB, Kjaer-Sorensen K, Overgaard MT, Weyer K, Poulsen CB, Sottrup-Jensen L, Conover CA, Giudice LC, Oxvig C. The Lin12-notch repeats of pregnancy-associated plasma protein-A bind calcium and determine its proteolytic specificity. *The Journal of biological chemistry* 2004;279(37):38525-31.
- [33] Samani AA, Yakar S, LeRoith D, Brodt P. The role of the IGF system in cancer growth and metastasis: overview and recent insights. *Endocrine reviews* 2007;28(1):20-47.
- [34] Yi HK, Hwang PH, Yang DH, Kang CW, Lee DY. Expression of the insulin-like growth factors (IGFs) and the IGF-binding proteins (IGFBPs) in human gastric cancer cells. *Eur J Cancer* 2001;37(17):2257-63.
- [35] Bodger K, Ahmed S, Pazmany L, Pritchard DM, Micheal A, Khan AL, Dimaline R, Dockray GJ, Varro A. Altered gastric corpus expression of tissue inhibitors of metalloproteinases in human and murine *Helicobacter* infection. *J Clin Pathol* 2008;61(1):72-8.
- [36] **Parsons BN, Ijaz UZ**, D'Amore R, Burkitt MD, Eccles R, Lenzi L, Duckworth CA, Moore AR, Tizslavicz L, Varro A, Hall N, Pritchard DM. Comparison of the human gastric microbiota in hypochlorhydric states arising as a result of *Helicobacter pylori*-induced atrophic gastritis, autoimmune atrophic gastritis and proton pump inhibitor use. *PLoS Pathog* 2017;13(11):e1006653.
- [37] Wang TC, Koh TJ, Varro A, Cahill RJ, Dangler CA, Fox JG, Dockray GJ. Processing and proliferative effects of human progastrin in transgenic mice. *Journal of Clinical Investigation* 1996;98(8):1918.
- [38] Luo W, Friedman MS, Shedden K, Hankenson KD, Woolf PJ. GAGE: generally applicable gene set enrichment for pathway analysis. *BMC bioinformatics* 2009;10:161.
- [39] Klopperpris S, Gaidamauskas E, Rasmussen LC, Overgaard MT, Kronborg C, Knudsen UB, Christiansen M, Kumar A, Oxvig C. A robust immunoassay for pregnancy-associated plasma protein-A2 based on analysis of circulating antigen: establishment of normal ranges in pregnancy. *Molecular human reproduction* 2013;19(11):756-63.
- [40] Lemos LM, Miyajima F, Castilho GR, Martins DTO, Pritchard DM, Burkitt MD. Hexane Extracts of *Calophyllum brasiliense* Inhibit the Development of Gastric Preneoplasia in *Helicobacter felis* Infected INS-Gas Mice. *Frontiers in Pharmacology* 2017;8.
- [41] Varro A, Dockray GJ, Bate GW, Vaillant C, Higham A, Armitage E, Thompson DG. Gastrin biosynthesis in the antrum of patients with pernicious anemia. *Gastroenterology* 1997;112(3):733-41.
- [42] Dockray GJ. Immunochemical studies on big gastrin using NH<sub>2</sub>-terminal specific antisera. *Regul Pept* 1980;1(3):169-86.

## Figure legends

**Figure 1.** Correlation heatmap of expression levels amongst all samples (A) and heatmap of the clustered  $\log_2$  fold change (FC) for differentially expressed genes (B). The 15 clusters are indicated by the red and blue bars. A gene's FC in expression level relative to time point W0 is indicated by heatmap colours. Each row represents a gene and regulation profile plot of significant clusters is expressed as FC. The expression of clusters 1 and 7 continued to increase after withdrawal of netazepide (C) and the expression of clusters 10, 13 and 14 decreased whilst the patients were taking netazepide but returned to pre-treatment levels after cessation of the drug. W0 = week 0/baseline, W6 = 6 weeks on netazepide, W12 = 12 weeks on netazepide and W24 = 12 weeks after cessation of netazepide treatment. Abbreviations are explained in Results section.

**Figure 2.** PAPPA2 mRNA expression was confirmed using qPCR in 8 patients with type-1 gNETs and 10 healthy control subjects. PAPPA2 mRNA expression significantly decreased whilst the gNET patients were taking 50mg oral daily dose of netazepide and returned to baseline after cessation of the treatment, in 12 week (A) and 12 month (B) studies. Statistical significance was determined using a Mann Whitney U test between independent healthy controls and baseline samples and a Wilcoxon signed rank test between repeated samples with Bonferroni correction for multiple comparisons, as not all the samples were normally distributed.  $P < 0.0125$  was considered significant after Bonferroni correction.  $*P < 0.0125$  and  $***P < 0.001$ . Immunohistochemical staining showed increased PAPPA2 and chromogranin A (ChgA) protein expression in serial histological sections of human micronodular ECL cell hyperplasia (C) and type-1 gNET tumor tissues (D). However, no significant differences in circulating PAPPA2 protein concentrations were observed between patients with hypergastrinemia and type-1 gNETs (n=8) (E) compared with healthy controls (n=10) (F).

**Figure 3.** Representative immunohistochemical staining for PAPPA2 in human gastric corpus biopsies from a patient who was taking netazepide for 12 weeks with a 12 week follow-up, then the same

patient on netazepide for a further 12 months. Increased PAPPA2 staining was observed only in samples when the patient was not taking netazepide.

**Figure 4.** PAPPA2 mRNA (A, B) and protein expression (C, D, E) were assessed using qPCR and immunofluorescence respectively and showed increases in expression in dose and time dependent manners following gastrin treatment. Maximal increases were observed after 10nM gastrin for 24h. Western blot for PAPPA2 in AGS<sub>GR</sub> cells treated with and without 10nM gastrin for 24h (F). Gastrin-stimulated PAPPA2 mRNA expression was completely reversed following pre-treatment with CCK2R antagonists YM022 (100nM) or netazepide (100nM) (G). Statistical significance was determined using either one-way ANOVA or two-way ANOVA where appropriate with Sidak *post hoc* test and  $P < 0.05$  was considered significant. \* $P < 0.05$ , \*\* $P < 0.01$ , \*\*\* $P < 0.001$  and \*\*\*\* $P < 0.0001$  vs untreated control at the same time point. Densitometry was performed using AxioVision Rel. 4.8 with the mean number of cells analysed  $132 \pm 13$  per treatment.

**Figure 5.** Gastrin treatment increased mouse gastric organoid area ( $\mu\text{m}^2$ ) (A) and PAPPA2 mRNA expression (B) and was maximal after 10nM gastrin for 24h. The increased organoid area and PAPPA2 mRNA expression caused by 10nM gastrin were completely reversed by pre-treatment with CCK2R antagonist drugs YM022 or netazepide (both 100nM) (C, D). Representative bright-field images were taken following 10nM gastrin treatment for 24hs with and without YM022 or netazepide pre-treatment (E). . Gastrin treatment also increased transgenic INS-GAS mouse derived gastric organoid area ( $\mu\text{m}^2$ ) and PAPPA2 mRNA expression after 10nM G17 for 24h. The increased organoid area and PAPPA2 mRNA expression caused by 10nM G17 was completely reversed by pre-treatment with CCK2R antagonist drugs YM022 or netazepide (both 100nM). Statistical significance was determined using two-way ANOVA with Sidak *post hoc* test and  $P < 0.05$  was considered significant. (\*\*\* $P < 0.001$  and \*\*\*\* $P < 0.0001$  vs 10nM gastrin positive control, ###  $P < 0.001$  and ####  $P < 0.0001$  vs untreated control).

**Figure 6.** Pre-treatment with either YM022 or netazepide at 100nM significantly reduced gastrin-induced PAPPA2 protein expression in 2D primary cell cultures derived from wild-type mouse gastric organoids. Densitometry was performed using AxioVision Rel. 4.8 on 3 reference fields per treatment (A). Representative images were taken per treatment (B). Statistical significance was determined using two-way ANOVA with Sidak *post hoc* test and  $P < 0.05$  was considered significant. \*\* $P < 0.01$  vs vehicle only control (DMSO 1%).

**Figure 7.** Circulating serum gastrin concentrations increased with age in transgenic INS-GAS mice and were significantly increased at 33 weeks of age compared with age-matched FVB/N control mice (A, B). Corpus histology showed no significant morphological changes in 15 week INS-GAS mice compared with age-matched FVB/N controls (C). However, extensive gastric tissue remodelling was observed in the corpus of 33 week old INS-GAS mice compared with age-matched wild-type mice (D). PAPPA2 mRNA expression was significantly increased in INS-GAS mice at 33 weeks, but not 15 weeks of age compared with age-matched FVB/N controls (E, F). Statistical significance was determined using student t-tests and  $P < 0.05$  was considered significant ( $n = 10$  mice per group), \*\* $P < 0.01$  and \*\*\* $P < 0.001$ .

**Figure 8.** Immunofluorescence and qPCR confirmed PAPPA2 (25nM) siRNA knockdown in AGS<sub>GR</sub> cells after 48h transfection, with a >80% reduction in protein expression (A, B) and >90% reduction in PAPPA2 mRNA (C). Densitometry was performed using AxioVision Rel. 4.8 with the mean number of cells analysed  $147 \pm 22$  per treatment. PAPPA2 siRNA knockdown significantly reduced the extension of long processes at 6h (D) and cell migration at 8h (E) induced by 10nM gastrin treatment. Representative images show changes in cell morphology (D) and migration (E) assays. Statistical significance was determined using either one-way ANOVA or two-way ANOVA where appropriate with Sidak *post hoc* test and  $P < 0.05$  was considered significant. \* $P < 0.05$ , and \*\*\*\* $P < 0.0001$  vs scrambled (25nM) control at the same time point. Recombinant PAPPA2 conditioned media (4 $\mu$ g/ml) increased AGS<sub>GR</sub> cell migration compared with untreated controls but was significantly less than

10nM G17 14h positive control (F). Statistical significance was determined using one-way ANOVA with Sidak *post hoc* test and  $P < 0.05$  was considered significant.  $**P < 0.01$  and  $****P < 0.0001$  vs vehicle control,  $\# P < 0.05$  and  $####P < 0.0001$ .

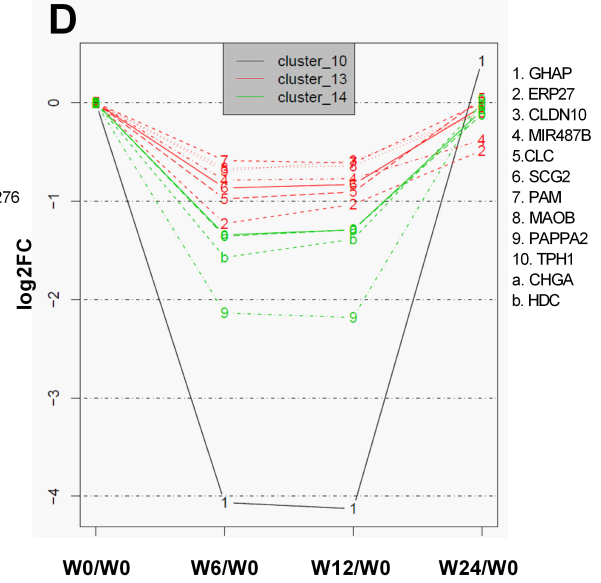
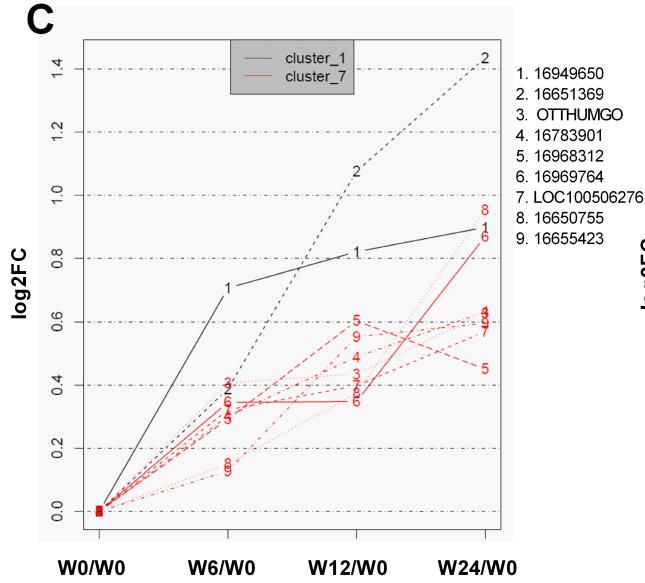
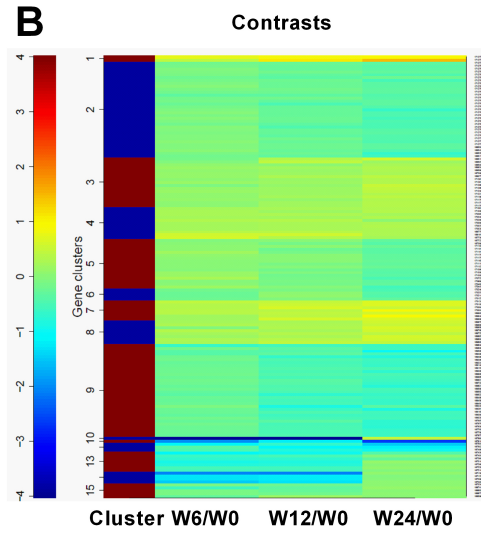
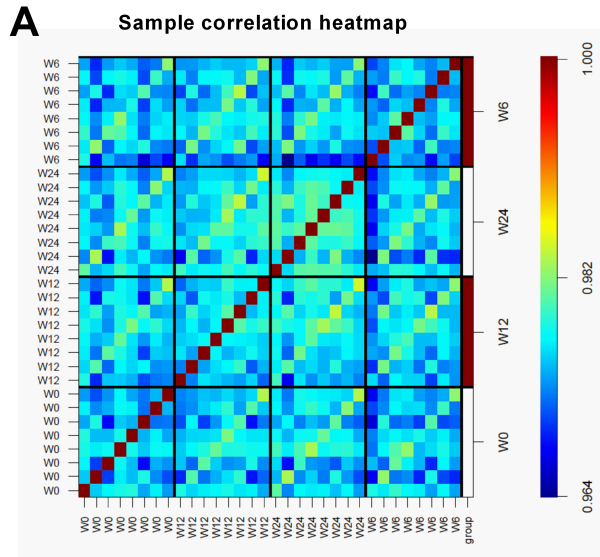
**Figure 9.** Gastrin treatment (10nM, 24h) increased the expression of IGFBP-5 and cleavage of IGFBP-3 (A, B) in the media of AGS<sub>GR</sub> cells. Experiments were performed in triplicate and statistical significance was determined using two-way ANOVA with Sidak *post hoc* test.  $*P < 0.05$  and  $**P < 0.01$ . Pre-treatment (20mins) with the IGF inhibitor, AG1024, further suppressed gastrin-induced migration (C, D) and extension of long processes (E, F) in AGS<sub>GR</sub> cells that have been transfected with 25nM PAPPA2 siRNA for 48h. Experiments were completed three times and statistical significance was determined using two-way ANOVA with Sidak *post hoc* test.  $P < 0.05$  was considered significant,  $****P < 0.0001$  scrambled 25nM siRNA+ 10nM gastrin vs no inhibitor.  $###P < 0.001$  and  $####P < 0.0001$  PAPPA2 25nM siRNA vs no inhibitor and  $+++P < 0.001$  and  $****P < 0.0001$  PAPPA2 25nM siRNA +10nM gastrin vs no inhibitor.

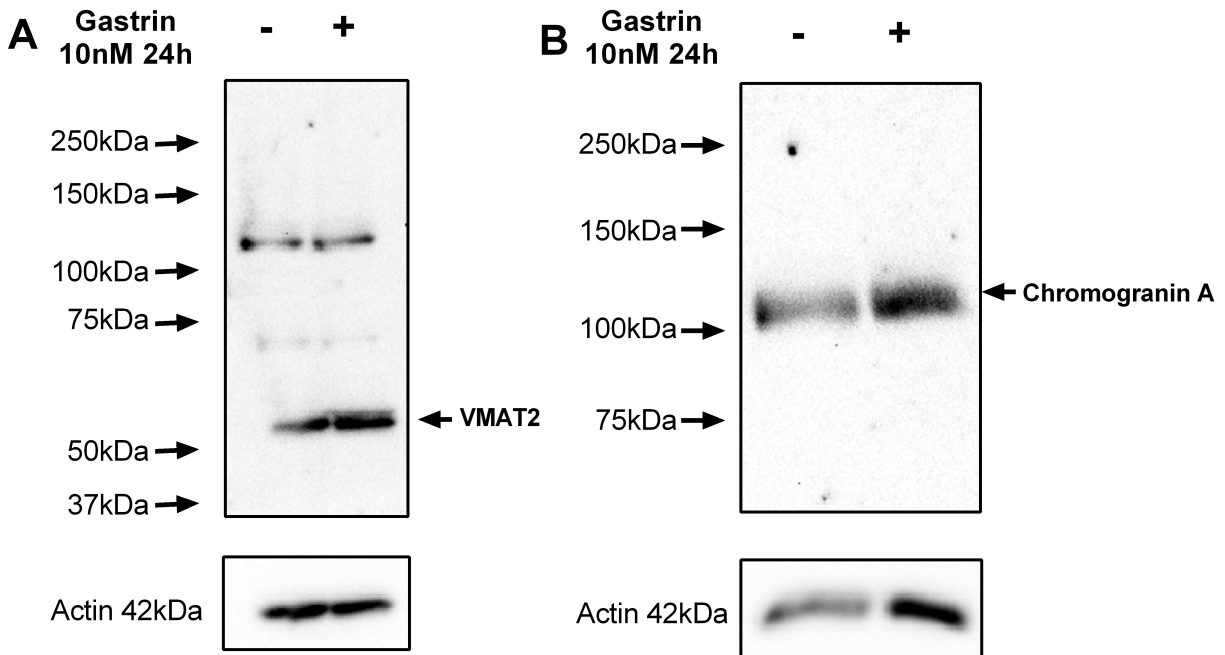
**Figure 10.** Western blots for (A) VMAT2 and (B) chromogranin A in AGS<sub>GR</sub> cells treated with and without 10nM gastrin for 24h.

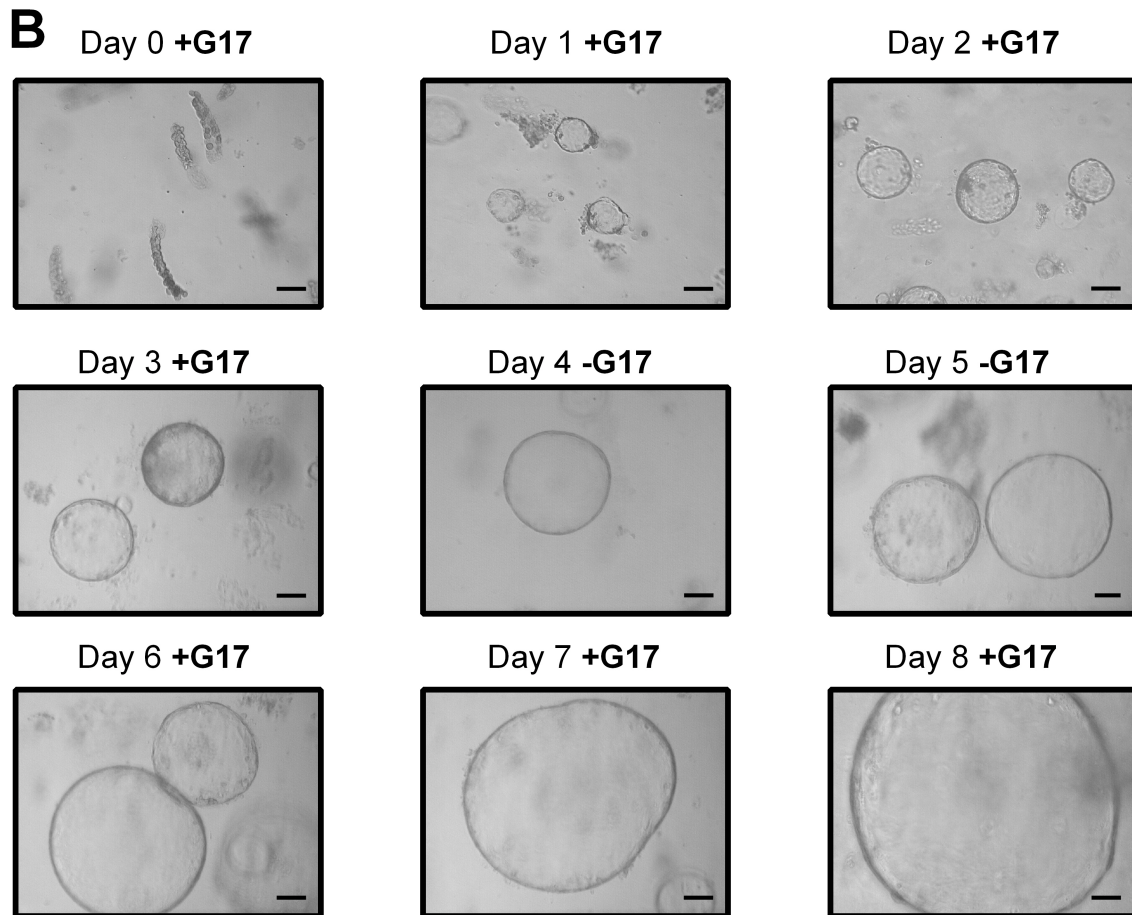
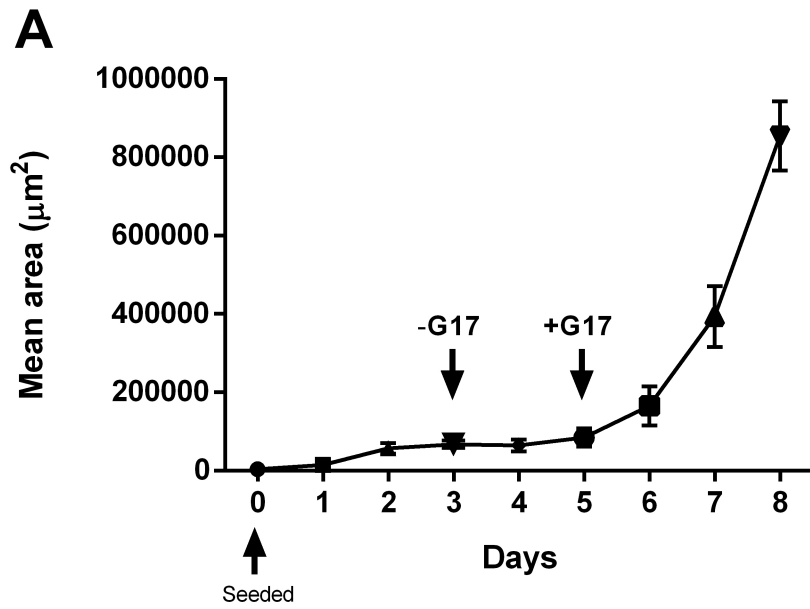
**Figure 11.** Organoids retain cell viability after removal of G17 for 48h, once G17 is reapplied. Organoids increased in area until the removal of 10nM G17 at day 3, when growth was inhibited. When 10nM G17 was then reapplied at day 5, gastric murine organoid area increased, time-dependently (A). Representative images are shown in (B).

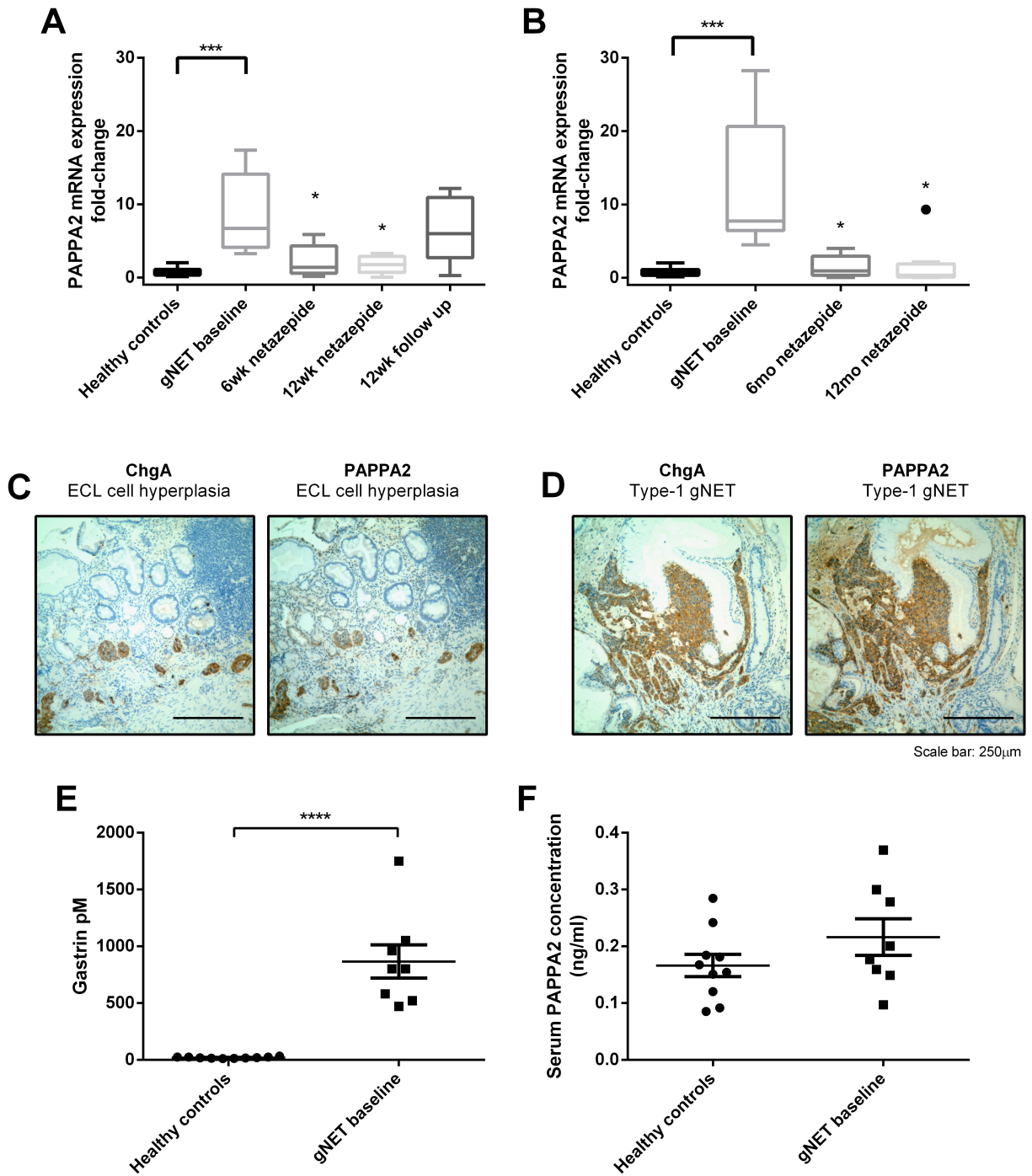
Table 1. Primer and small interfering RNA (siRNA) sequences

Target gene	Type	Sequence
PAPP-A2	Forward primer	GCATCTCAGCTGTGGCTCTA
PAPP-A2	Reverse primer	AGTTACTGGGAGCCGAAAGAC
GAPDH	Forward primer	CAGCAAGAGCACAAGAGGAA
GAPDH	Reverse primer	GTGGTGGGGACTGAGTGT
PAPP-A2	siRNA pool	CAUCAUCGCAGGUGUGUUU GCCCAAGCAUCCCUUAAA GGGCUCCGUUCACCAACUA CAAGAGGGCAUACAUGAGU
Non-targeting (scrambled)	siRNA pool	UGGUUUACAUGUCGACUAA UGGUUUACAUGUUGUGUGA UGGUUUACAUGUUUUCUGA UGGUUUACAUGUUUCCUA

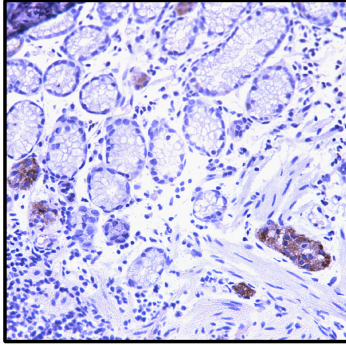




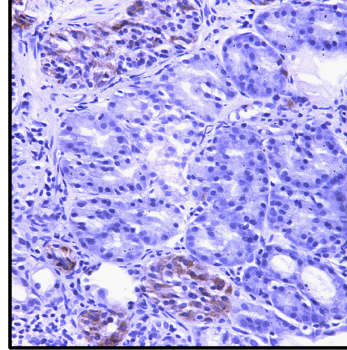




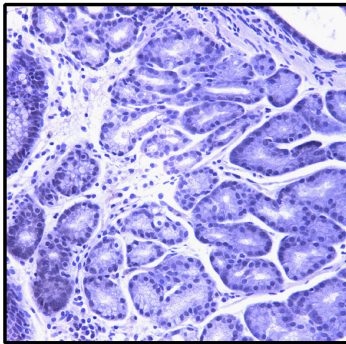
(A) Baseline 1



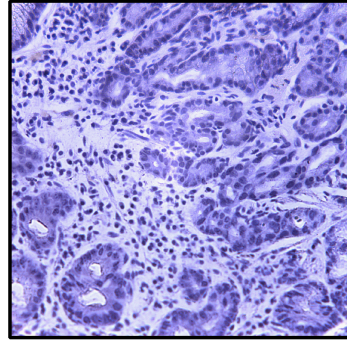
(E) Baseline 2



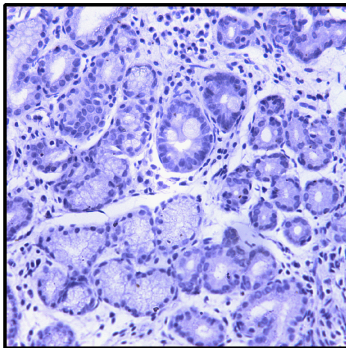
(B) 6 weeks on netazepide



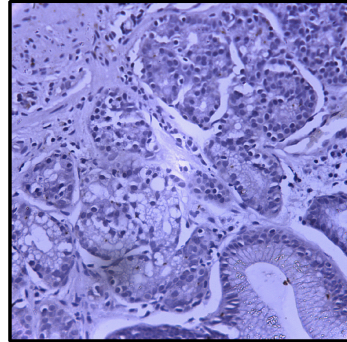
(F) 6 months on netazepide



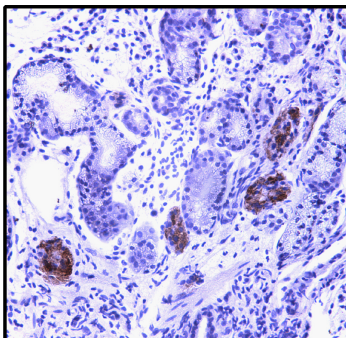
(C) 12 weeks on netazepide

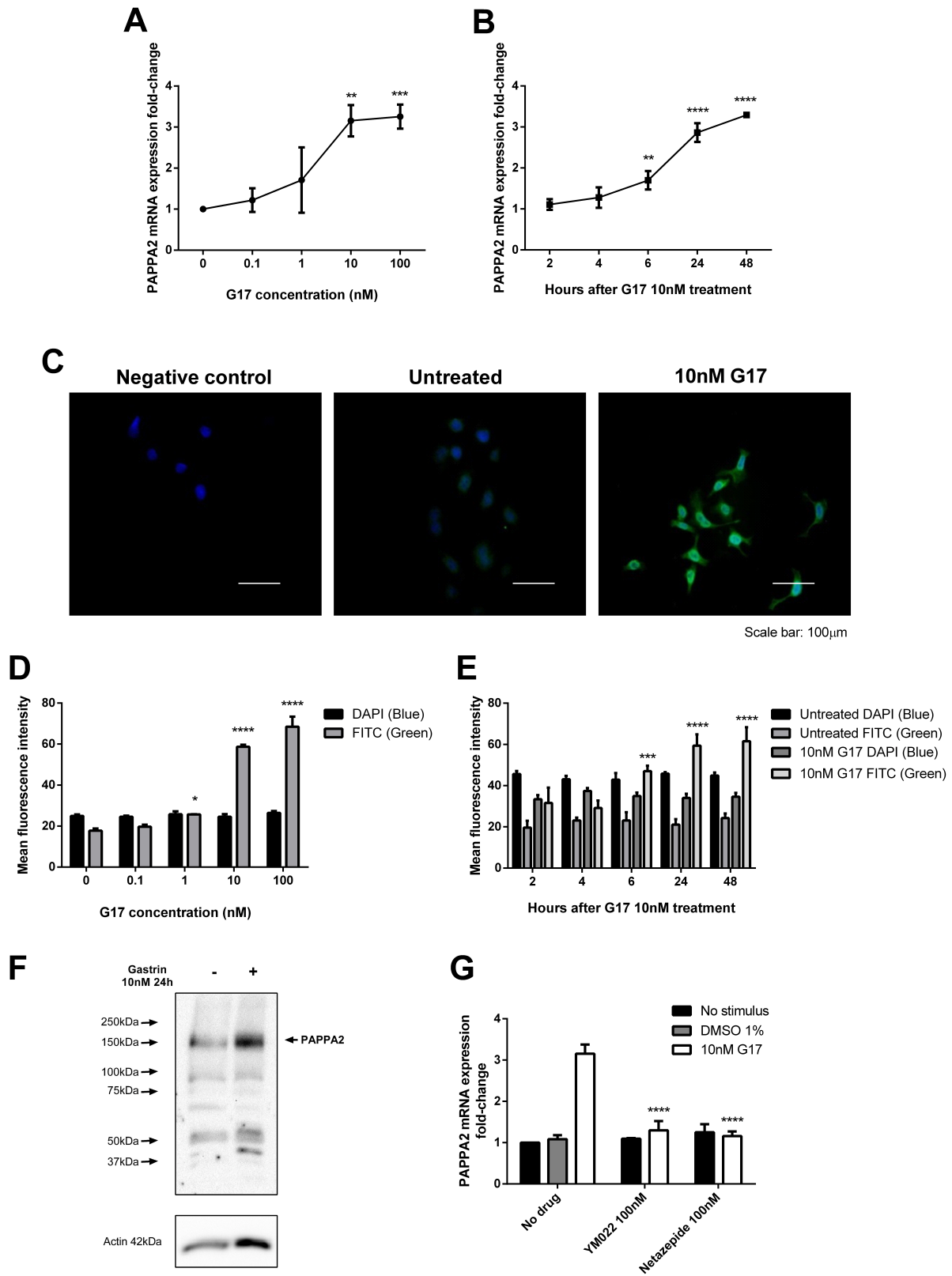


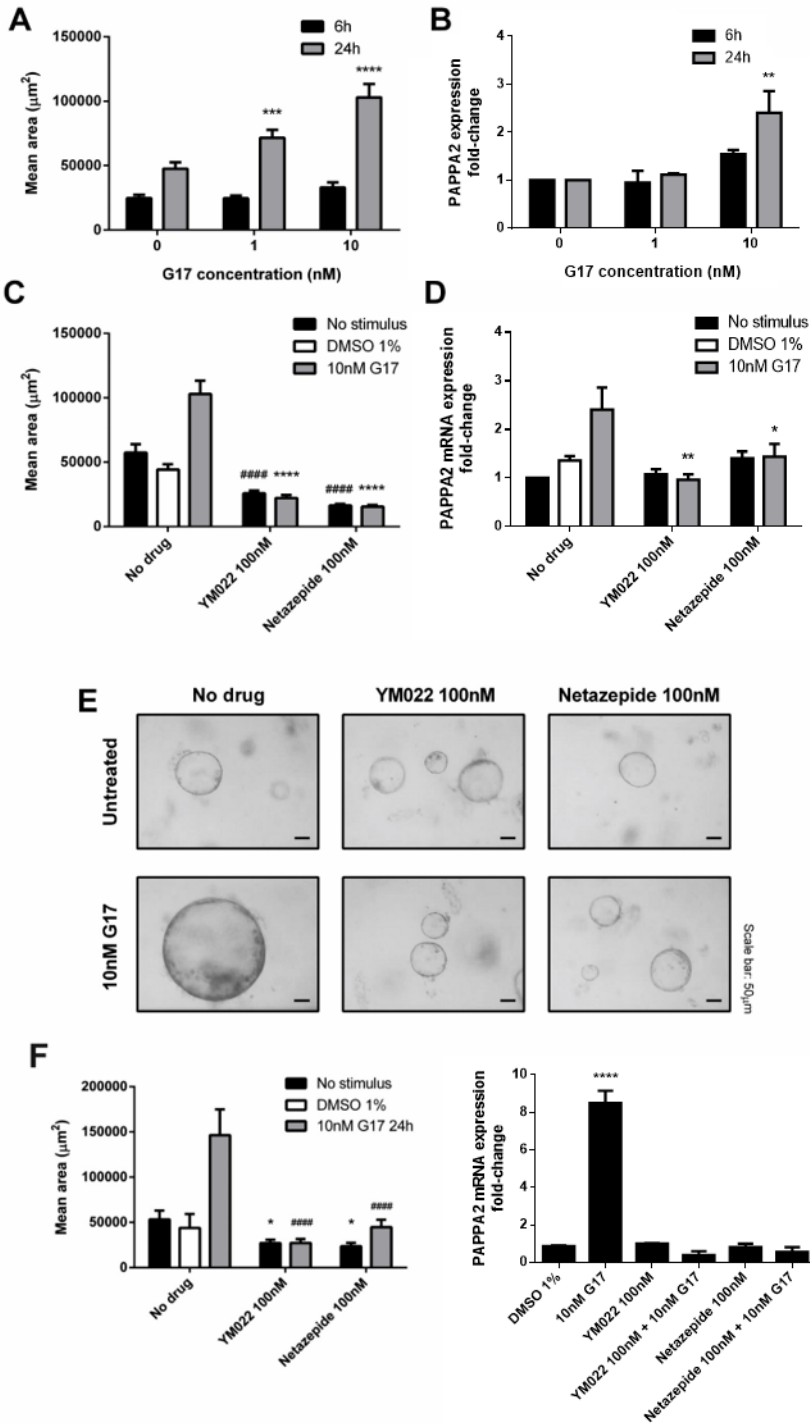
(G) 12 months on netazepide

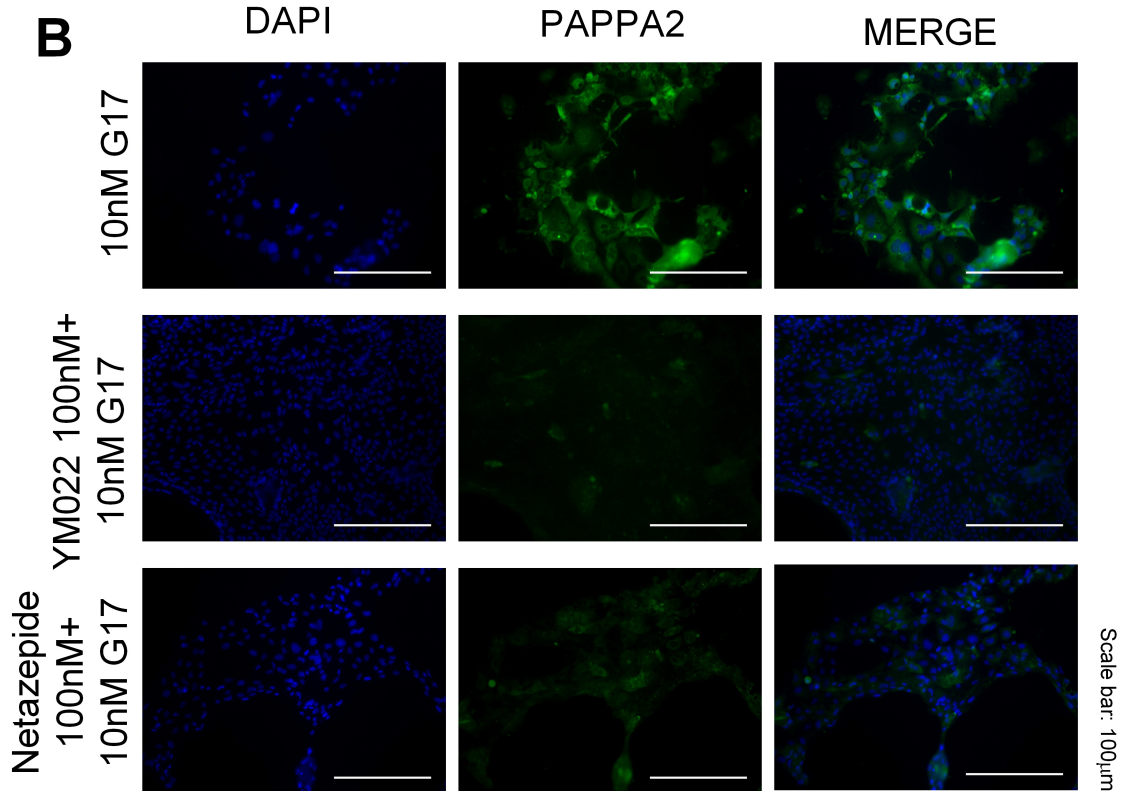
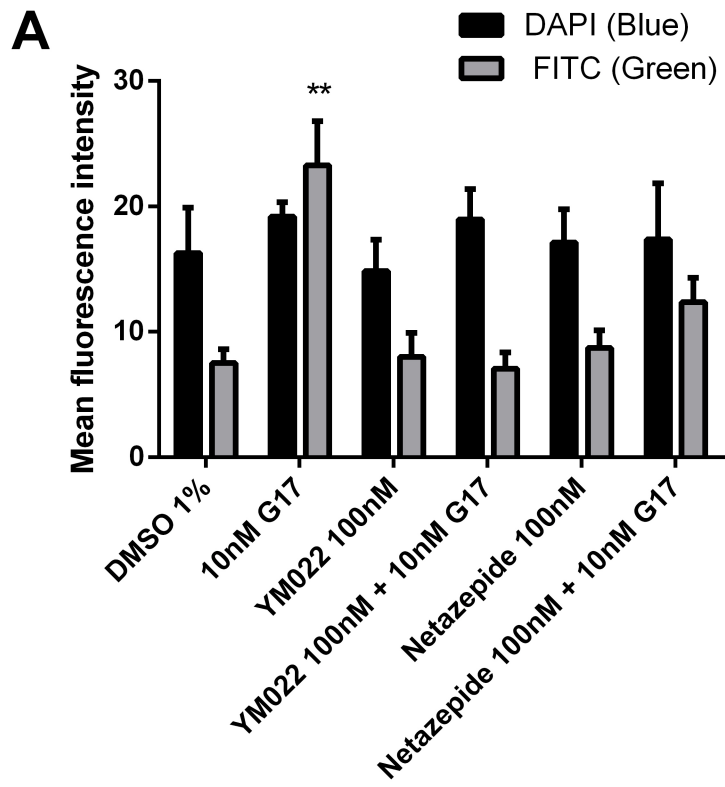


(D) 12 weeks after netazepide

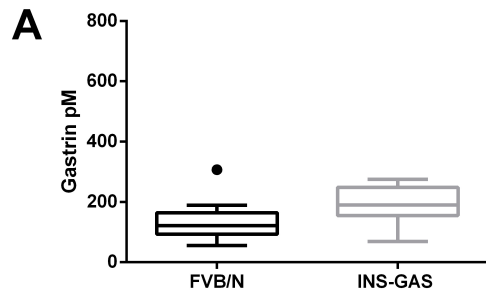




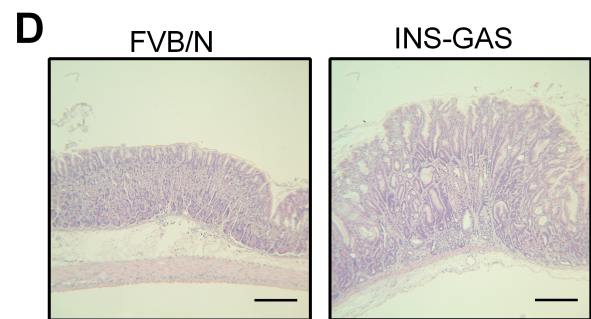
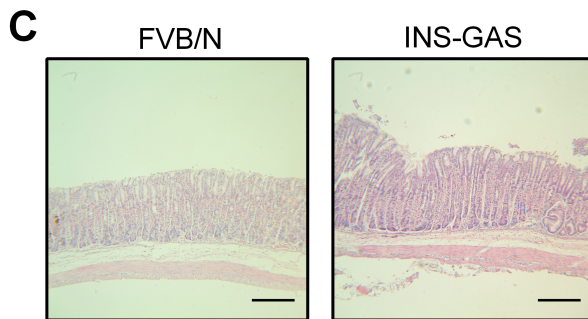
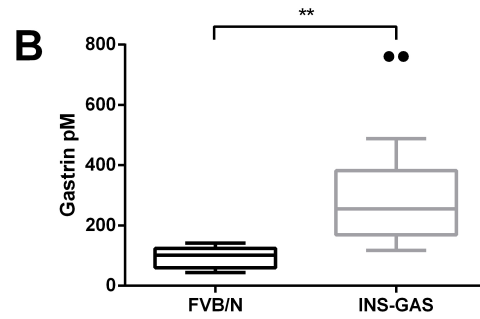
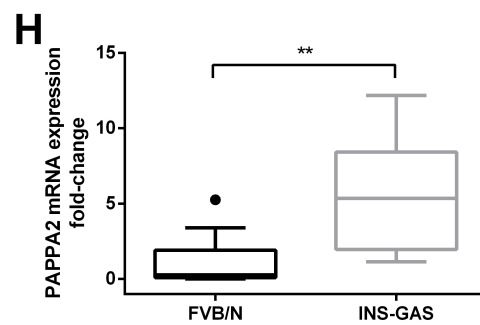
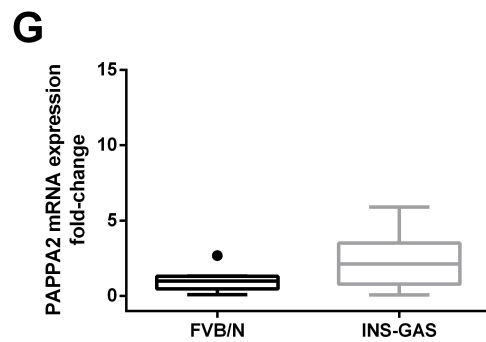
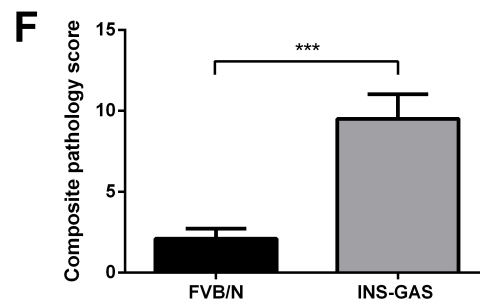
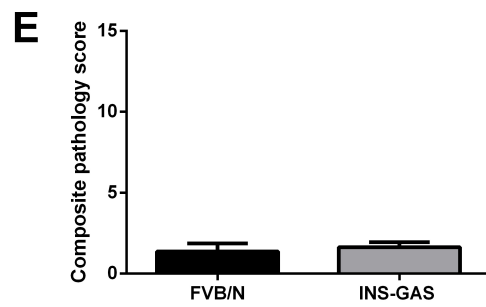


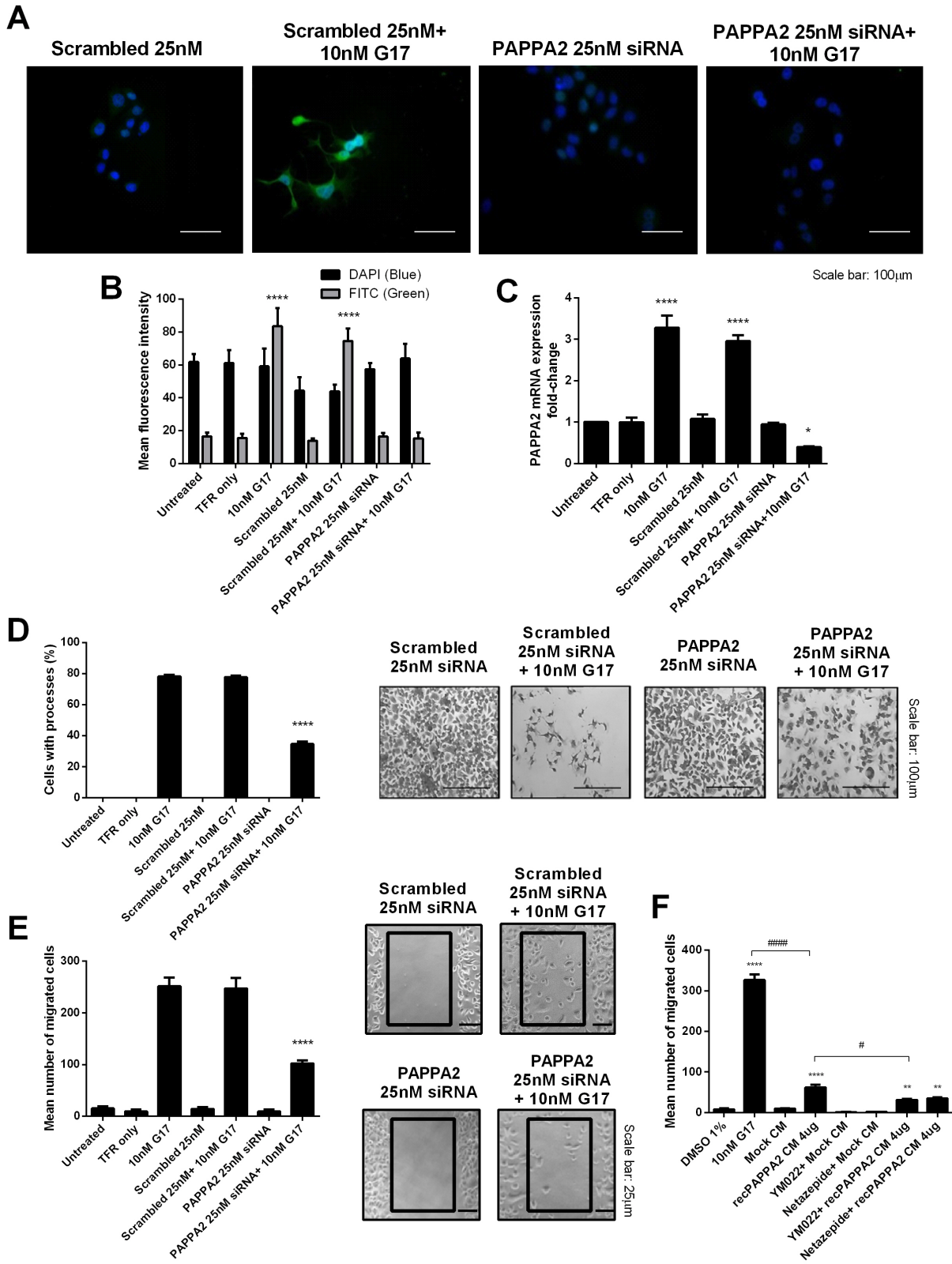


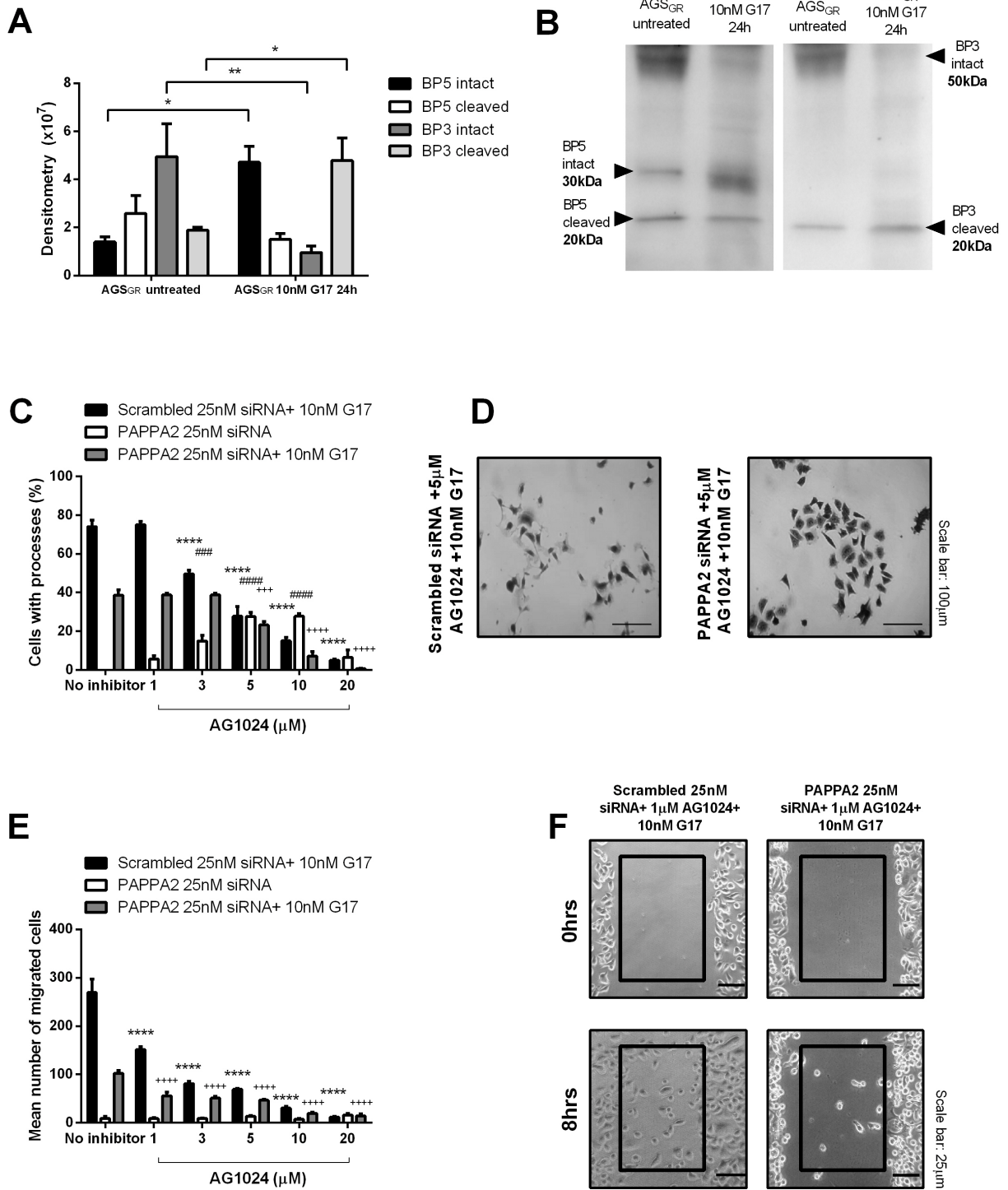
15 weeks



33 weeks

Scale bar: 250 $\mu$ m





ID	gene_assignment	logFC.W06vW0	logFC.W12vW0	logFC.W24vW0	PV.W06vW0	PV.W12vW0	PV.W24vW0	FDR.W06vW0	FDR.W12vW0	FDR.W24vW0
17021437	NM_001252383 // CGA // glycoprotein hormones, alpha	-4.065	-4.1275	0.42875	1.40E-11	1.02E-11	0.221224	7.50E-07	5.47E-07	0.648238
16787650	ENST00000216492 // CHGA // chromogranin A (parathyroid hormone-related protein)	-1.34125	-1.29125	-0.0775	1.52E-09	3.13E-09	0.591458	4.08E-05	5.60E-05	0.86733
16674151	ENST00000367662 // PAPA2 // pappalysin 2 // 1q23-q24	-2.1375	-2.1825	0.02875	3.13E-09	2.11E-09	0.90398	5.59E-05	5.60E-05	0.975284
16809075	ENST00000267845 // HDC // histidine decarboxylase // 1q21-q22	-1.57125	-1.38625	-0.01	8.38E-09	7.81E-08	0.956818	0.0001123	0.000838	0.989862
16888554	ENST00000304698 // FAM171B // family with sequence similarity 171B	-0.63625	-0.385	0.03625	6.88E-07	0.000491	0.707995	0.0073796	0.1966	0.912656
17110289	NM_000898 // MAOB // monoamine oxidase B // Xp11.23	-0.665	-0.64125	-0.1	8.27E-07	1.46E-06	0.332583	0.007392	0.006516	0.734164
16736405	ENST00000250018 // TPH1 // tryptophan hydroxylase 1	-1.355	-1.29125	-0.11625	1.81E-06	3.73E-06	0.596678	0.0139006	0.009935	0.869293
16872248	NM_001828 // CLC // Charcot-Leyden crystal galectin // 1q21-q22	-0.97625	-0.90625	0.04375	2.47E-06	7.33E-06	0.786072	0.0148801	0.01511	0.941824
16908977	NM_003469 // SCG2 // secretogranin II // 2q35-q36 // 7q31-q32	-0.865	-0.83	-0.04	2.50E-06	4.60E-06	0.77958	0.0148801	0.01072	0.939356
16761830	ENST00000266397 // ERP27 // endoplasmic reticulum protein 27	-1.2275	-1.0325	-0.4825	3.07E-06	3.38E-05	0.025982	0.0164602	0.040303	0.323822
16775844	NM_182848 // CLDN10 // claudin 10 // 13q31-q34 // 90	-0.69375	-0.58625	-0.09875	4.45E-06	4.40E-05	0.410404	0.0200888	0.048178	0.780982
16987673	NM_000919 // PAM // peptidylglycine alpha-amidating lyase	-0.58625	-0.61125	0.0025	4.50E-06	2.42E-06	0.980196	0.0200888	0.008122	0.995195
17118854	---	-0.35625	0.1225	-0.03375	5.02E-06	0.056086	0.585374	0.0207183	0.611378	0.865218
16972299	---	-0.4	-0.38375	-0.48	6.16E-06	1.10E-05	3.77E-07	0.0220298	0.018503	0.001262
16654237	---	0.54375	0.30125	0.17375	6.16E-06	0.00394	0.078298	0.0220298	0.379884	0.469535
16859821	---	0.3375	0.32875	0.2275	9.21E-06	1.32E-05	0.000935	0.0308645	0.020296	0.103899
16801108	NM_013243 // SCG3 // secretogranin III // 15q21 // 2910	-0.83	-0.7425	0.05625	1.70E-05	7.10E-05	0.720104	0.0536092	0.069821	0.916975
16788758	NR_030267 // MIR487B // microRNA 487b // 14q32.31 // 7	-0.78625	-0.77	-0.3775	1.84E-05	2.43E-05	0.017406	0.0547337	0.031408	0.282208
16651791	---	0.535	0.5275	0.2325	2.08E-05	2.51E-05	0.0311	0.0588309	0.031408	0.345804
16811762	NM_006715 // MAN2C1 // mannosidase, alpha, class 2C	0.2525	0.0825	-0.005	2.33E-05	0.100691	0.918461	0.0625128	0.680755	0.979086
16970185	OTTHUMT00000365381 // OTTHUMG00000161575 // N	-0.46625	-0.18	0.02125	2.66E-05	0.057298	0.815657	0.0680353	0.613402	0.950894
16817713	NR_015396 // CDIPT-AS1 // CDIPT antisense RNA 1 (hepatocellular carcinoma)	0.41375	0.1375	-0.01125	2.80E-05	0.099676	0.889744	0.0681265	0.68046	0.971463
16875683	ENST00000412770 // PPP6R1 // protein phosphatase 6, regulatory, cytosolic	0.27625	0.22125	0.04875	3.00E-05	0.000402	0.374727	0.0698789	0.177814	0.757836
16701119	NM_152666 // PLD5 // phospholipase D family, member 5	-0.625	-0.3875	-0.17	3.80E-05	0.004653	0.183796	0.0825287	0.385021	0.613293
16781268	NM_000705 // ATP4B // ATPase, H <sup>+</sup> /K <sup>+</sup> exchanging, beta 4	-1.7	-0.66375	0.065	4.07E-05	0.062404	0.849851	0.0825287	0.625753	0.959991
16940161	NM_001837 // CCR3 // chemokine (C-C motif) receptor 3	-0.545	-0.36875	-0.19875	4.11E-05	0.002445	0.08062	0.0825287	0.333783	0.47444
16713971	---	-0.7275	-0.62625	-0.69125	4.23E-05	0.000248	7.96E-05	0.0825287	0.141412	0.040241
16911201	NM_001819 // CHGB // chromogranin B (secretogranin 2)	-0.69	-0.45625	-0.0025	4.52E-05	0.003137	0.9858	0.0825287	0.353565	0.996542
17101392	NM_015691 // WWC3 // WWC family member 3 // Xp22.3	0.29125	0.16125	0.16125	4.58E-05	0.011262	0.011262	0.0825287	0.457512	0.242495
16938654	OTTHUMT00000342017 // KRT18P15 // NULL // --- // ---	0.26	0.315	-0.01875	4.62E-05	3.33E-06	0.723968	0.0825287	0.009658	0.918571
17127643	---	-0.52375	-0.875	-1.04375	0.000682977	9.75E-07	5.23E-08	0.1717959	0.006516	0.000458
17127399	---	-0.32	-0.52625	-0.67375	0.001389214	3.89E-06	7.46E-08	0.1923949	0.009935	0.000458
17118177	AK293868 // LOC100506276 // uncharacterized LOC100506276	0.32125	0.3975	0.56875	0.001489452	0.000174	1.44E-06	0.1970613	0.116327	0.003515
17127243	---	-0.33	-0.5825	-0.6725	0.001556865	1.63E-06	1.62E-07	0.2006597	0.006637	0.000671
17127615	---	-0.275	-0.50125	-0.57	0.001892035	1.40E-06	1.77E-07	0.2134814	0.006516	0.000677
17127245	---	-0.295	-0.57125	-0.71875	0.002063564	6.35E-07	1.25E-08	0.2160046	0.005678	0.000223
17127357	---	-0.30875	-0.54625	-0.67875	0.002197378	2.87E-06	8.77E-08	0.2193981	0.009059	0.00047
17127259	---	-0.31375	-0.54	-0.70375	0.002438917	5.17E-06	7.68E-08	0.2249837	0.011544	0.000458
17127653	---	-0.31875	-0.61375	-0.69875	0.00289944	1.32E-06	1.63E-07	0.2409295	0.006516	0.000671

17127623 ---	-0.31	-0.59375	-0.62125	0.00338513	1.93E-06	9.58E-07	0.2530747	0.006889	0.002568
17127639 ---	-0.46125	-1.19	-1.245	0.003678373	1.59E-08	6.98E-09	0.2564588	0.000214	0.000223
17127641 ---	-0.275	-0.50625	-0.60125	0.005194594	7.84E-06	5.86E-07	0.2747662	0.015333	0.001848
17127241 ---	-0.24375	-0.50875	-0.645	0.005337581	1.29E-06	2.45E-08	0.2755703	0.006516	0.000263
17127665 ---	-0.29875	-0.52625	-0.62	0.006010807	1.90E-05	1.81E-06	0.2812287	0.027472	0.003958
17127631 ---	-0.33375	-0.50875	-0.85	0.006426881	0.00013	7.54E-08	0.2823899	0.103829	0.000458
17127649 ---	-0.30625	-0.54	-0.65125	0.007043481	2.52E-05	1.76E-06	0.2845896	0.031408	0.003958
16740406 AF001542 // MALAT1 // metastasis associated lung ader	-0.17375	-0.365	-0.53375	0.01081025	5.46E-06	1.06E-08	0.3163827	0.011717	0.000223
17127619 ---	-0.2575	-0.56125	-0.77375	0.011147064	3.42E-06	1.73E-08	0.3180741	0.009658	0.000232
16968312 ---	0.2925	0.6025	0.45	0.011313769	8.01E-06	0.0003	0.3192686	0.015333	0.073221
17127621 ---	-0.2425	-0.485	-0.56625	0.015049327	2.26E-05	2.54E-06	0.3414726	0.031111	0.004865
17127661 ---	-0.31	-0.68125	-0.9075	0.032278069	4.18E-05	6.89E-07	0.4254762	0.046739	0.002052
17127627 ---	-0.23625	-0.415	-0.66375	0.03589421	0.000668	1.85E-06	0.4380495	0.205219	0.003958
17127683 ---	-0.23375	-0.58	-0.775	0.036790449	1.21E-05	1.40E-07	0.439291	0.019616	0.000671
17109121 ---	-0.13875	-0.3225	-0.415	0.048243835	6.23E-05	1.94E-06	0.46729	0.063069	0.003976
16651369 ---	0.3875	1.07625	1.435	0.120192905	0.000157	3.65E-06	0.5899671	0.114164	0.006556
17117798 ---	-0.11875	-0.41	-0.485	0.157136587	3.70E-05	3.67E-06	0.6380305	0.042236	0.006556
16816171 ---	0.09375	-0.11625	-0.46	0.217706599	0.129567	2.00E-06	0.6928285	0.710531	0.003976
17002871 ---	-0.09	-0.52	-0.5425	0.288588014	1.73E-06	8.99E-07	0.7457694	0.006637	0.002536
17117542 ---	-0.08625	-0.325	-0.52625	0.299733533	0.000533	1.08E-06	0.7517997	0.198494	0.002747
17127659 ---	-0.13625	-0.9225	-0.43375	0.354740078	1.30E-06	0.006132	0.7845256	0.006516	0.203327
17118171 ENST00000331523 // EEF1A1 // eukaryotic translation el	-0.07125	-0.31375	-0.6175	0.420092156	0.001389	2.34E-07	0.8203002	0.278114	0.000835

Journal Pre-proof

## Down regulated known genes

ID	gene_assignment	logFC.W06vW0	logFC.W12vW0	logFC.W24vW0	PV.W06vW0	PV.W12vW0	PV.W24
17021437	NM_001252383 // CGA // glycoprotein hormones, alpha polypeptide // 6q12-q21 // 1081 /// NM_000735 // CGA // glycoprotein hormones, alpha polypeptide // 6q12-q21 // 1081 /// ENST00000369582 // CGA // glycoprotein hormones, alpha polypeptide // 6q12-q21 // 1081 /// BC010957 // CGA // glycoprotein h	-4.065	-4.1275	0.42875	1.3997E-11	1.01961E-11	0.2212
16674151	ENST00000367665 // PAPA2 // pappalysin 2 // 1q23-q25 // 60676 /// NM_020318 // PAPA2 // pappalysin 2 // 1q23-q25 // 60676 /// ENST00000367661 // PAPA2 // pappalysin 2 // 1q23-q25 // 60676 /// BC152552 // PAPA2 // pappalysin 2 // 1q	-2.1375	-2.1825	0.02875	3.12894E-09	2.10983E-09	9.9039
17018525	NM_001832 // CLPS // colipase, pancreatic // 6p21.31 // 1208 /// NM_001252597 // CLPS // colipase, pancreatic // 6p21.31 // 1208 /// ENST00000259938 // CLPS // colipase, pancreatic // 6p21.31 // 1208 /// NM_001252598 // CLPS // colipase, pancreatic // 6p21.31 // 1208 /// BC025693 // CLPS // colipase, pancr	-2.2025	-1.64125	-1.61125	5.81766E-05	0.001346981	0.0015
16809073	ENST00000267845 // HDC // histidine decarboxylase // 15q21-q22 // 3067 /// NM_002112 // HDC // histidine decarboxylase // 15q21-q22 // 3067 /// M60445 // HDC // histidine decarboxylase // 15q21-q22 // 3067 /// BC130527 // HDC // histidine decarboxylase // 15q21-q22 // 3067 /// BC144173 // HDC // histid	-1.57125	-1.38625	-0.01	8.37669E-09	7.81498E-08	9.9568
17090713	NM_001807 // CEL // carboxyl ester lipase // 9q34.3 // 1056 /// ENST00000372080 // CEL // carboxyl ester lipase // 9q34.3 // 1056 /// M85201 // CEL // carboxyl ester lipase // 9q34.3 // 1056	-1.71875	-1.3025	-1.5825	0.000753364	0.007441033	0.0016
16659637	NM_015849 // CELA2B // chymotrypsin-like elastase family, member 2B // 1p36.21 // 51032 /// ENST00000375910 // CELA2B // chymotrypsin-like elastase family, member 2B // 1p36.21 // 51032 /// BC069455 // CELA2B // chymotrypsin-like elastase family, member 2B // 1p36.21 // 51032 /// BC113540 // CELA2B	-2.09	-1.3	-2.75125	0.001436378	0.034698326	8.0301
16787650	ENST00000216492 // CHGA // chromogranin A (parathyroid secretory protein 1) // 14q32 // 1113 /// NM_001275 // CHGA // chromogranin A (parathyroid secretory protein 1) // 14q32 // 1113 /// BC006459 // CHGA // chromogranin A (parathyroid secretory protein 1) // 14q32 // 1113 /// ENST00000553866 // CH	-1.34125	-1.29125	-0.0775	1.523E-09	3.13267E-09	0.5914
16736405	ENST00000250018 // TPH1 // tryptophan hydroxylase 1 // 11p15.3-p14 // 7166 /// NM_004179 // TPH1 // tryptophan hydroxylase 1 // 11p15.3-p14 // 7166 /// BC106739 // TPH1 // tryptophan hydroxylase 1 // 11p15.3-p14 // 7166 /// ENST00000341556 // TPH1 // tryptophan hydroxylase 1 // 11p15.3-p14 // 7166	-1.355	-1.29125	-0.11625	1.8148E-06	3.73431E-06	0.5966
16667850	NM_000699 // AMY2A // amylase, alpha 2A (pancreatic) // 1p21 // 279 /// ENST00000414303 // AMY2A // amylase, alpha 2A (pancreatic) // 1p21 // 279 /// BC007060 // AMY2A // amylase, alpha 2A (pancreatic) // 1p21 // 279 /// ENST00000497748 // AMY2A // amylase, alpha 2A (pancreatic) // 1p21 // 279	-1.855	-1.135	-1.76125	0.002356345	0.048376443	0.0035
16761830	ENST00000266397 // ERP27 // endoplasmic reticulum protein 27 // 12p12.3 // 121506 /// NM_152321 // ERP27 // endoplasmic reticulum protein 27 // 12p12.3 // 121506 /// BC030218 // ERP27 // endoplasmic reticulum protein 27 // 12p12.3 // 121506	-1.2275	-1.0325	-0.4825	3.06996E-06	3.3826E-05	0.025
17051601	NM_001868 // CPA1 // carboxypeptidase A1 (pancreatic) // 7q32 // 1357 /// ENST0000011292 // CPA1 // carboxypeptidase A1 (pancreatic) // 7q32 // 1357 /// AK291493 // CPA1 // carboxypeptidase A1 (pancreatic) // 7q32 // 1357 /// BC005279 // CPA1 // carboxypeptidase A1 (pancreatic) // 7q32 // 1357 /// BTC	-1.43375	-1.01625	-1.67625	0.004095333	0.033960519	0.0010
16872248	NM_001828 // CLC // Charcot-Leyden crystal galectin // 19q13.1 // 1178 /// ENST00000221804 // CLC // Charcot-Leyden crystal galectin // 19q13.1 // 1178 /// L01664 // CLC // Charcot-Leyden crystal galectin // 19q13.1 // 1178	-0.97625	-0.90625	0.04375	2.47305E-06	7.32724E-06	0.7860
17051536	ENST00000222481 // CPA2 // carboxypeptidase A2 (pancreatic) // 7q32 // 1358 /// NM_001869 // CPA2 // carboxypeptidase A2 (pancreatic) // 7q32 // 1358 /// BC007009 // CPA2 // carboxypeptidase A2 (pancreatic) // 7q32 // 1358 /// ENST00000416698 // CPA2 // carboxypeptidase A2 (pancreatic) // 7q32 // 135	-1.27875	-0.85625	-1.74	0.004747405	0.048026347	0.0002
16976561	ENST00000446444 // UGT2B11 // UDP glucuronosyltransferase 2 family, polypeptide B11 // 4q13.2 // 10720 /// ENST00000513315 // UGT2B11 // UDP glucuronosyltransferase 2 family, polypeptide B11 // 4q13.2 // 10720	-0.75875	-0.83625	-0.54	0.001629372	0.00065719	0.0185
16961487	NM_000340 // SLC2A2 // solute carrier family 2 (facilitated glucose transporter), member 2 // 3q26.1-q26.2 // 6514 /// ENST00000314251 // SLC2A2 // solute carrier family 2 (facilitated glucose transporter), member 2 // 3q26.1-q26.2 // 6514 /// J03810 // SLC2A2 // solute carrier family 2 (facilitated glucose transp	-0.85875	-0.83375	-0.49	0.009762915	0.011795195	0.1223
16908977	NM_003469 // SCG2 // secretogranin II // 2q35-q36 // 7857 /// ENST00000305409 // SCG2 // secretogranin II // 2q35-q36 // 7857 /// BC022509 // SCG2 // secretogranin II // 2q35-q36 // 7857 /// ENST00000421386 // SCG2 // secretogranin II // 2q35-q36 // 7857 /// ENST00000433889 // SCG2 // secretogranin II //	-0.865	-0.83	-0.04	2.49773E-06	4.59846E-06	0.7795
16788739	NR_030266 // MIR376A2 // microRNA 376a-2 // 14q32.31 // 664615	-0.64125	-0.825	-0.83	0.010319451	0.001505251	0.0014

## Upregulated known genes

17051370	NR_002187 // TP1P2 // triosephosphate isomerase 1 pseudogene 2 // 7q32.1 // 286016 /// AK094894 // TP1P2 // triosephosphate isomerase 1 pseudogene 2 // 7q32.1 // 286016	0.22875	0.50375	0.18125	0.151881985	0.003319196	0.2524
16916531	OTTHUMT00000077567 // OTTHUMG0000031681 // NULL // --- // OTTHUMT00000077567 // RPS-96811.1 // NULL // --- // ---	0.41375	0.51125	0.2925	0.019365432	0.004915074	0.0891
16797583	AF067420 // IGH A1 // immunoglobulin heavy constant alpha 1 // 14q32.33 // 3493 /// BC073782 // IGHG1 // immunoglobulin heavy constant gamma 1 (G1m marker) // 14q32.33 // 3500 /// ENST00000454421 // IGHV3-64 // immunoglobulin heavy variable 3-64 // --- // ---	0.2725	0.51125	0.38875	0.019432172	8.85996E-05	0.0015
16797667	NR_040094 // CT60 // cancer/testis antigen 60 (non-protein coding) // 15q11.2 // 348120 /// ENST00000553416 // CT60 // cancer/testis antigen 60 (non-protein coding) // 15q11.2 // 348120	0.43125	0.515	0.1375	0.018437252	0.005917762	0.428
16882790	ENST00000390278 // IGVK1D-42 // immunoglobulin kappa variable 1D-42 (non-functional) // --- // ---	0.19625	0.52375	-0.0675	0.197583535	0.001677309	0.652
16807761	NR_036195 // MIR4310 // microRNA 4310 // --- // 100423013	0.50625	0.525	0.35375	0.003300161	0.002300195	0.906
16964831	NR_039961 // MIR4798 // microRNA 4798 // --- // 100616471	0.17	0.53875	0.67125	0.493111945	0.037197857	0.0111
17012140	ENST00000363440 // RNASSP215 // RNA, 5S ribosomal pseudogene 215 // --- // ---	0.2275	0.5475	0.3475	0.365951503	0.036268042	0.1720
16703603	ENST00000494304 // LYZL1 // lysozyme-like 1 // 10p12.1 // 84569	0.38375	0.555	0.3225	0.049521893	0.006322471	0.0949
16927752	ENST00000390298 // IGLV7-43 // immunoglobulin lambda variable 7-43 // --- // ---	0.26	0.5575	0.4475	0.182573316	0.007089367	0.0265
16782028	ENST00000390489 // TRAI48 // T cell receptor alpha joining 48 // --- // ---	0.3025	0.59625	0.5475	0.054601134	0.000548071	0.0012
16921823	ENST00000410986 // RNASSP489 // RNA, 5S ribosomal pseudogene 489 // --- // ---	0.02125	0.6275	-0.3725	0.935706483	0.024102246	0.1658
16724715	NM_024114 // TRIM48 // tripartite motif containing 48 // 11q11 // 79097 /// ENST00000417545 // TRIM48 // tripartite motif containing 48 // 11q11 // 79097 /// AF521869 // TRIM48 // tripartite motif containing 48 // 11q11 // 79097	0.445	0.65	0.20375	0.123355486	0.028364121	0.471
16797542	BC009851 // IGHM // immunoglobulin heavy constant mu // 14q32.33 // 3507 /// ENST00000390621 // IGHV1-45 // immunoglobulin heavy variable 1-45 // --- // ---	0.7675	0.705	0.3125	0.009325925	0.015824426	0.261
16750595	NM_012404 // ANP32D // acidic (leucine-rich) nuclear phosphoprotein 32 family, member D // 12q13.11 // 23519 /// ENST00000266594 // ANP32D // acidic (leucine-rich) nuclear phosphoprotein 32 family, member D // 12q13.11 // 23519 /// BC069122 // ANP32D // acidic (leucine-rich) nuclear phosphoprotein 32	0.29625	0.745	0.62375	0.180244313	0.001974177	0.0077
16781997	ENST00000390474 // TRDJ4 // T cell receptor delta joining 4 // --- // ---	0.715	0.78875	0.74375	0.022915305	0.013048713	0.0184
16948835	NR_030410 // MIR1224 // microRNA 1224 // 3q27.1 // 100187716	0.75375	0.895	0.41125	0.039320846	0.016123459	0.2460

Journal Pre-proof